Bjerrums Foredrag Nr. 21

Knut H. Andersen

Bearing capacity under cyclic loading – offshore, along the coast, and on land.

Utgitt av

LAURITS BJERRUMS MINNEFOND

Norsk Geoteknisk Forening

Oslo 2009

Laurits Bjerrums Minneforedrag

Nr. 1 6. februar 1975
"Formation and Geotechnical Characteristics of Glacial-Lake Varved Soils"
by T.Cameron Kenney

Nr. 2 14. mars 1977
"Deformation computations in Geotechnical Engineering""
av Kaare Høeg

Nr. 3 27. februar 1978
"Deformation Behaviour of Soils in Terms of Soil Moduli"
av Oddvin Tokheim

Nr. 4 19. mars 1979
"A Geotechnical Engineer's 7th Sense"
av Elmo DiBiagio

Nr. 5 5. mai 1980
"Where Has All The Judgement Gone?"
by Ralph B. Peck

Nr. 6 15. mars 1982
"Is Limit State Design a Judgement Killer?"
by Knud Mortensen

Nr. 7 7. mars 1983
"En vegs geotekniske liv"
av Geir Refsdal (ikke publisert)

Nr. 8 4. mars 1985
"Deformation phenomena in jointed rock"
by Nick Barton (ikke publisert)

Nr. 9 21 april 1986
"Small is beautiful – the stiffness of soils at small strains"
by John B. Burland

Nr. 10 16. mars 1987
"Udrenert skjærstyrke som funksjon av effektive spenninger"
av Gunnar Aas (ikke publisert)

Nr. 11 11. april 1998
"Grundförstarkning av gamla hus med stålrörspålar"
av Håkan Stille (ikke publisert)

Nr. 12 17. april 1989
"Norsk geoteknikk 1950-75
Tilbakeblikk med refleksjoner"
Av Håkon Hartmark, Gudrun Bjerrum, Ove Eide, Jan Friis, Bjørn Kjærnsli, og Nilmar Janbu

Nr. 13 29. april 1991
"A case history of mysterious settlements in a building"
by James M. Duncan

Nr. 14 3. mars 1993
"Snow avalanche experience through 20 years"
av Karstein Lied

Nr. 15 15. mars 1995
"Laurits Bjerrums fornemmelse for utstyr"
av Arild Aa. Andresen

Nr. 16 23. september 1998
"Fundamentering av plattformer, observasjoner og refleksjoner"
av Carl J. Frimann Clausen

Nr. 17 5. april 2000
"Eurocode 7 og geoteknikerens hverdag"
av Niels Krebs Ovesen (ikke publisert)

Nr. 18 24. april 2002
"Forurensning av grunnen – et spørsmål om naturens bæreevne"
av Gijs D. Breedveld

Nr. 19 21. november 2003
"Laurits Bjerrum – more than an engineer"
av Kaare Flaate

Nr. 20 25. November 2005
"The magic of sands"
av David Muir Wood

Nr. 21 23. November 2007
"Bearing capacity under cyclic loading - offshore, along the coast, and on land"
av Knut H. Andersen

Bjerrums Foredrag Nr. 21

Knut H. Andersen

Bearing capacity under cyclic loading – offshore, along the coast, and on land.

Utgitt av

LAURITS BJERRUMS MINNEFOND

Norsk Geoteknisk Forening

Oslo 2009

Bearing capacity under cyclic loading - offshore, along the coast and on land

The 21st Bjerrum Lecture, presented in Oslo 23 November 2007

Knut H. Andersen

Technical Director, Norwegian Geotechnical Institute (NGI)

ABSTRACT

Cyclic loading can be important for the foundation design of structures, both offshore, along the coast and on land, and for the stability of slopes. This is illustrated by several examples. The paper discusses how soil behaves under cyclic loading, both for structures and for slopes, and shows that the cyclic shear strength and the failure mode under cyclic loading depend strongly on the stress path and the combination of average and cyclic shear stresses. Diagrams with cyclic shear strength of clay, sand and silt that can be used in practical design are presented. Comparisons between calculations and model tests indicate that foundation capacity under cyclic loading can be determined on the basis of cyclic shear strength determined in laboratory tests.

INTRODUCTION

Bearing capacity under cyclic loading is governing for the foundation design of offshore installations, and cyclic soil behaviour has received significant attention over the last 30-40 years. However, there are also installations and slopes along the coast and on land where it is important to consider effects of cyclic loading on bearing capacity.

At NGI, the study of behaviour of soils under cyclic loading started in the early 1970-ies in connection with the first exploitation of oil and gas in the North Sea. Dr. Laurits Bjerrum, NGI's director at that time, saw the geotechnical challenges in connection with the foundation design of the fixed platforms that were to be constructed, and he enthusiastically involved NGI in practical foundation design and research in this area (e.g. Bjerrum, 1973). Since then, the cyclic behaviour of soil has been an important topic at NGI.

The paper first gives examples of cases where cyclic loading is important for foundation design. Then it explains how soil behaves under cyclic loading, and diagrams with cyclic shear strength of clay, silt and sand that can be used in practical design are provided. Finally, comparisons of calculated to measured bearing capacity in model tests are shown, indicating that bearing capacity under cyclic loading can be reliably predicted based on cyclic strength from laboratory tests.

EXAMPLES OF CYCLIC LOADING

The first gravity platform in the North Sea was the Ekofisk Oil Storage Tank in Figure 1, which was installed in June 1973 (Clausen *et al.*, 1975). The tank was designed for a 100-year storm with a maximum wave of 24 m. In addition to the maximum wave, the foundation had to withstand the forces from a large number of other waves in the storm. These forces may generate excess pore pressure and degrade the soil prior to the impact of the maximum wave.

Note: Published in Can. Geotech. J. 46: 513-535 (2009)

Figure 1. The Ekofisk Oil Storage Tank, installed in the North Sea in June 1973 (based on Clausen et al., 1975).

Figure 2. The Frigg TCP2 Condeep platform in the North Sea (adapted from Andersen and Høeg, 1991).

Since the installation of the Ekofisk Tank a large number of gravity platforms have been installed in the North Sea and other parts of the world. In several cases, the platforms have been designed for severe storms with a maximum 100-year wave in excess of 30 m. One example is the Frigg TCP2 Condeep platform in Figure 2.

In recent years, gravity platforms have also been designed to serve as LNG terminals. These terminals have been situated closer to land than the installations for oil and gas production. Geotechnically, this has presented new challenges with soil profiles consisting of mixed layers of loose silt, sand and soft clay often significantly less uniform than encountered further offshore.

Essentially all offshore installations will experience wave loading and need to be designed for cyclic loading. In addition to the gravity platforms mentioned above, this includes piled installations, anchors and skirted installations. One example is the Snorre TLP platform, which in 1991 was the first tension leg installation to be anchored by means of suction anchors (Christophersen *et al.*, 1992) (Figure 3). Due to the novelty of the suction anchor concept at that time, extensive studies

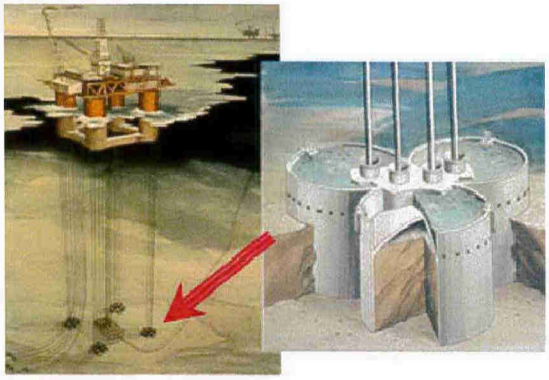

Figure 3. The Snorre TLP platform installed in the North Sea in 1991.

Figure 4. Suction anchors installed at the Horn Mountain field in the Gulf of Mexico in 2002 (photo by E.C. Clukey, BP America Production Company).

were made to ensure that the foundation design methods were sound. This included field model testing that are described towards the end of this paper. Suction anchors have since been extensively used to anchor various types of floating installations. An example is shown in Figure 4. By the end of 2004, about 500 suction anchors were installed at 50 different offshore locations worldwide in water depths reaching more than 2000 m (Andersen *et al.*, 2005).

Figure 5. The Oosterschelde Storm Surge Barrier. (http://www.deltawerken.com/Deltaworks, photo by the Ministry of Public Works, Transport and Water Management, The Netherlands).

Figure 6. Offshore wind turbines (http://www.vestas.com).

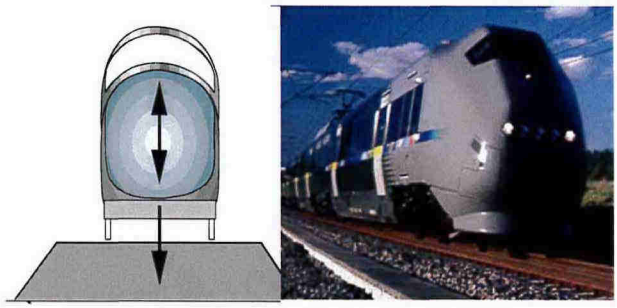

Figure 7. Vibrations from traffic (photo: Christian Madshus, NGI).

Structures along the coast may also be subjected to severe wave loading. Such structures include harbours, breakwaters and storm surge barriers. One example is the Oosterschelde storm surge barrier in the Netherlands that was completed in 1986 (Figure 5).

Many wind turbines are now placed offshore (Figure 6), and their foundation needs to be designed for cyclic loading

from both wind and waves. Even if placed on land, they do of course need to be designed for cyclic wind loading.

On land there are also situations with cyclic loading. This includes design of road and railway embankments and cuts for effects from traffic-induced cyclic loading (Figure 7). In seismic areas, earthquakes may cause foundation failures of buildings and bridges (Figure 8) and induce slope failures (Figure 9). Cyclic loading from traffic and earthquakes have lower cyclic load periods (~1s) than wave loading (~10-20s) and this needs to be taken into account.

Ice loading can cause cyclic loads on structures that are placed in the sea. The Great Belt bridge in Denmark, for instance (Figure 10), was designed for cyclic loading from ice sheets that break when they float past and impact on the bridge piers (Andersen *et al.*, 1991). Andersen et al. (1991) reported that breaking of the ice sheet would cause an impulse that set the bridge piers in motion with a frequency determined by their resonance periods. This would lead to a two-frequency cyclic loading on the soil beneath the piers (Figure 10). The importance of ice loading on offshore structures will increase as the oil and gas production moves into arctic areas.

WHAT HAPPENS TO SOIL SUBJECTED TO CYCLIC LOADING?

General behaviour

Cyclic loading may reduce the bearing capacity of a soil, and the bearing capacity under cyclic loading may be lower than the capacity under monotonic loading. This is illustrated by the results of model tests of a gravity platform on clay in Figure 11. The model has a submerged weight,

Figure 8. Earthquake damage on buildings (photo: Amir Kaynia, NGI).

Figure 9. Earthquake induced landslide, El Salvador (U.S. Geological Survey/from photo by Ed Harp, USGS).

W', and is loaded with a cyclic horizontal load, H_{cy}, a distance z above the seafloor. The results show that the displacements under cyclic loading increase with number of cycles and become larger than the displacements under monotonic loading at the same load. The model develops excessive displacements and fails at a cyclic load that is lower than the failure load under monotonic loading.

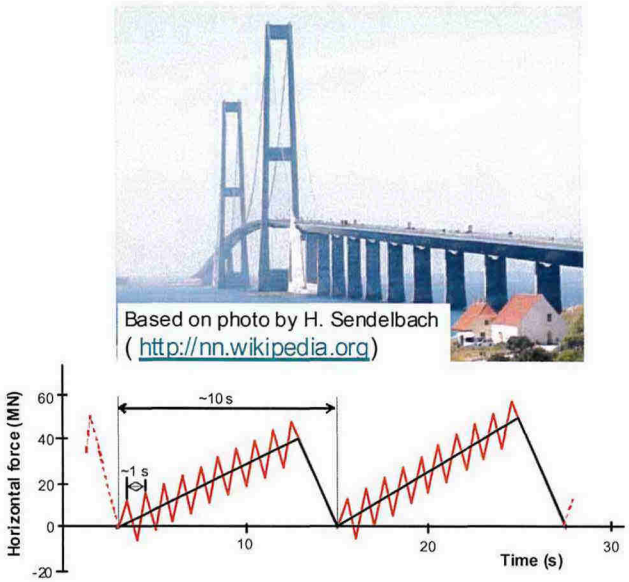

Figure 10. Ice load history for Great Belt bridge piers.

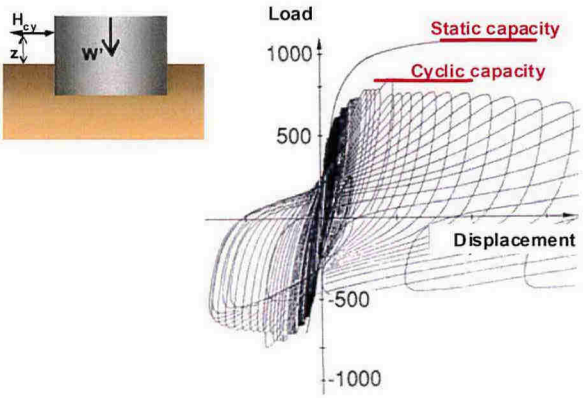

Figure 11. Results of model tests with monotonic and cyclic loading on gravity platform on clay based on (Andersen et al., 1989).

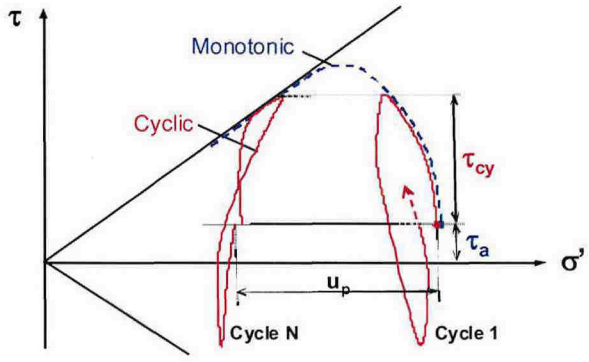

Figure 12. Effective stress paths for undrained tests with monotonic and cyclic loading.
u_p= permanent pore-pressure component; σ'= effective normal stress; τ = shear stress. τ_a= average shear stress; τ_{cy} = single-amplitude cyclic shear stress;

In this paper, the failure load and the shear stress at failure under monotonic loading will be called static capacity and static shear strength, respectively.

The reason why the cyclic capacity may be smaller than the static capacity is that the cyclic loading tends to break down the soil structure and cause a tendency for volumetric reduction in the soil. If the conditions are undrained, volumetric changes will be prevented by the low volumetric compressibility of the water. The normal stresses that were carried by the soil will then be transferred to the pore water and the effective stresses in the soil will decrease accordingly. This is illustrated by the effective stress paths for monotonic and cyclic soil elements in Figure 12.

The development of pore pressure and shear strain with time for a soil element subjected to undrained cyclic loading with a constant cyclic shear stress is illustrated in Figure 13. The load cycles with a single amplitude shear stress, τ_{cy}, around a constant shear stress, τ_a. The cyclic loading generates a pore pressure characterized by a permanent pore pressure component, u_p, and a cyclic pore pressure component, u_{cy}. The increased pore pressure reduces the effective stresses in the soil, resulting in increased permanent, γ_p, and cyclic, γ_{cy}, shear strains with time.

The stress-strain behaviour of a soil element under the cyclic loading in Figure 13 is illustrated in Figure 14.

Effect of average shear stress and test type

The soil beneath a structure is subjected to various stress conditions where the average and cyclic shear stresses and the

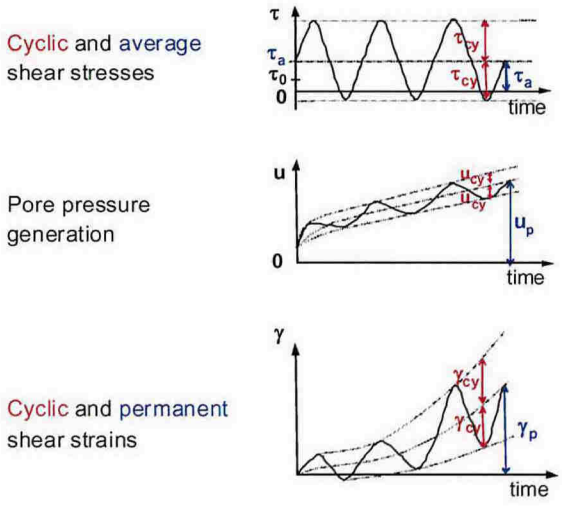

Figure 13. Pore pressure and shear strain as function of time under undrained cyclic loading.

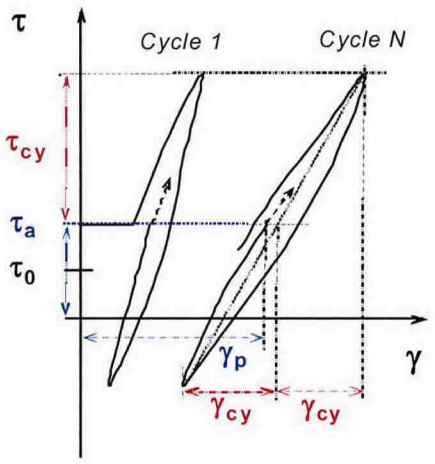

Figure 14. Stress-strain behaviour under cyclic loading.

type of loading (e.g. triaxial vs. direct simple shear, DSS) vary from one point to another. This is illustrated in Figure 15, which shows a simplified picture of the stress conditions along a potential failure surface beneath a gravity structure under cyclic loading.

The behaviour of soil elements under various loading conditions is illustrated in Figures 16 and 17 with results from laboratory tests on Drammen Clay, a marine clay with a plasticity index of I_p=27%.

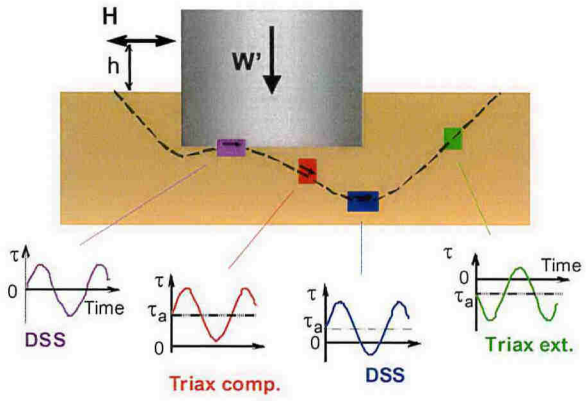

Figure 15. Simplified stress conditions along a potential failure surface in the soil beneath a gravity structure under cyclic loading. H = resultant horizontal load; h= height above seafloor of resultant horizontal load.

The first two tests in Figure 16, Figures 16a and 16b, show that the response to symmetrical cyclic loading is different in DSS and triaxial tests. In the DSS tests, the shear strain develops relatively symmetrically, apart from the first quarter cycle. In the triaxial test, the shear strain is non-symmetrical with a permanent shear strain of the same magnitude as the cyclic shear strain. This is related to the strength anisotropy under triaxial loading, with an extension strength that is smaller than the compression strength. The third test in Figure 16c has a shear stress where the average and the cyclic components are the same. The result is a shear strain development with dominant permanent shear strain and small cyclic shear strain which does not increase significantly with number of cycles. Figure 17 shows that the cyclic behaviour is not governed by the maximum shear stress. The three tests in Figure 17 have the same maximum shear stress, but different average and cyclic shear stress components. The test with τ_a=0 fails after 10 cycles, whereas the tests with τ_a=0.5·τ_{max} and τ_a=0.85·τ_{max} have developed only small shear strains after 2500 cycles, and the test with the highest τ_a has the smallest shear strains.

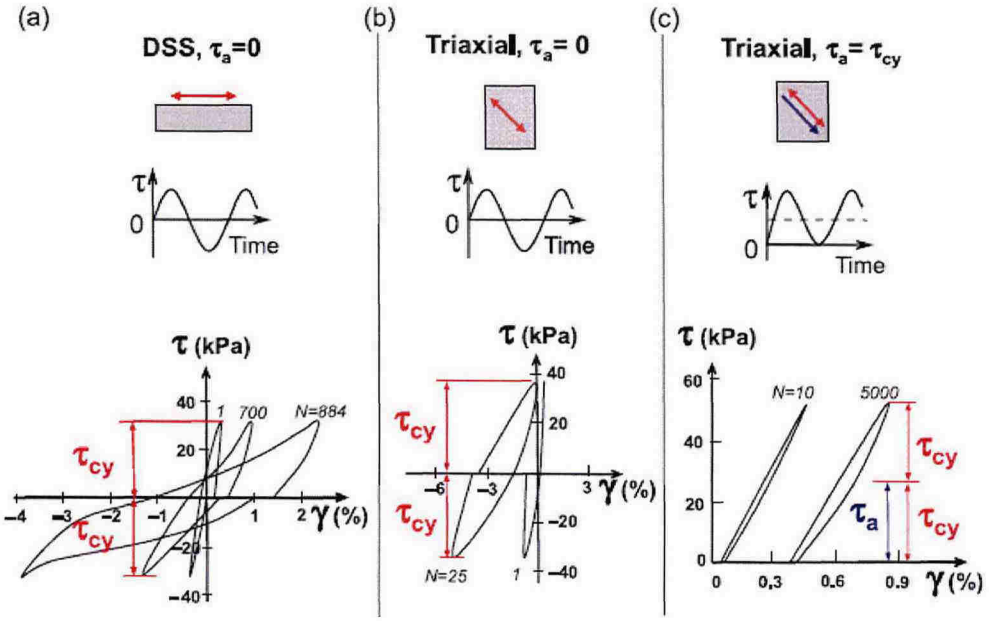

Figure 16. Stress-strain behaviour under various cyclic loading conditions.

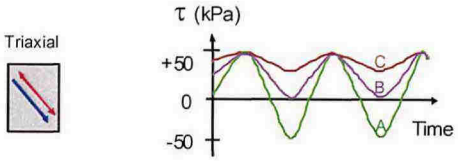

Test	τ_{max}	τ_a	τ_{cy}	Result
A	50	0	50	Failure (γ=15%) 10 cycles
B	50	25	25	γ_p=0.8%, γ_{cy}=0.3% 2500 cycles
C	50	42.5	7.5	γ_p=0.03%, γ_{cy}=0.02% 2500 cycles

Figure 17. Results from cyclic triaxial tests with same maximum shear stress.

These examples illustrate that the cyclic behaviour depends on both average and cyclic shear stresses, and that the behaviour is different in triaxial and DSS tests. The next section describes how this knowledge can be utilized to establish design diagrams for practical applications.

Number of cycles to failure as function of average and cyclic shear stresses

Given the importance of the average and cyclic shear stress components for the cyclic behaviour, the results from a large DSS and triaxial cyclic testing programme on plastic Drammen Clay (e.g. Andersen *et al.*, 1988) were plotted as function of average and cyclic shear stresses.

The plot for DSS tests on normally consolidated clay is presented in Figure 18. The left hand plot shows the results from 1 monotonic and 9 cyclic tests. The location of the various points is determined by the average and cyclic shear stresses under which the tests were run, and the numbers along each point give the number of cycles to failure, N_f, and the permanent and cyclic shear strains at failure, γ_p/γ_{cy}. Failure was defined as either a permanent or a cyclic shear strain of 15%. The shear stresses are in Figure 18 normalized with respect to the static shear strength, s_u, in a DSS test run to failure with a constant rate of shear strain of ~4.5%/hour.

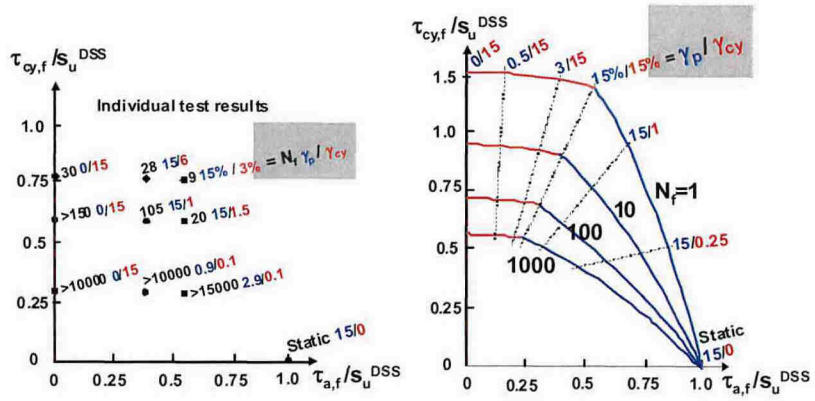

Figure 18. Number of cycles to failure and failure mode as function of average and cyclic shear stresses for cyclic DSS tests on normally consolidated Drammen Clay. (a) Results from one monotonic and nine cyclic tests; (b) contour diagram with the same number of cycles to failure based on the data in part (a). $\tau_{a,f}$ = average shear stress at failure; $\tau_{cy,f}$, cyclic shear stress at failure; s_u = static DSS shear strength.

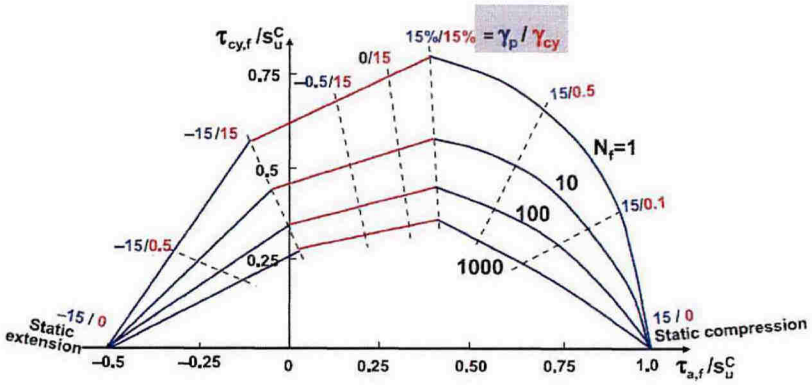

Figure 19. Number of cycles to failure and failure mode as function of average and cyclic shear stresses for cyclic triaxial tests on normally consolidated Drammen Clay.

By inspection of the data in the diagram on the left hand side of Figure 18, it was possible to draw contours through points with the same number of cycles to failure. This gave the contour diagram on the right hand side of Figure 18. Curves that define the failure mode, i.e. the permanent and cyclic shear strains at failure, are drawn in addition.

The contour diagram defines the number of cycles to failure as function of average and cyclic shear stresses. The diagram also defines the failure mode; i.e. the combination of permanent and cyclic shear strains at failure, γ_p and γ_{cy}. The diagram shows that the failure will occur as large cyclic shear strains when the average shear stress is small, and as large permanent shear strains when the average shear stress approaches the static shear strength. For average shear stresses between zero and the static shear strength, the failure mode will be a combination of permanent and cyclic shear strains.

A contour diagram similar to the one for DSS tests is given for triaxial tests in Figure 19. The diagram is established based on a number of cyclic triaxial tests, each with different average and cyclic shear stresses, like for the DSS tests. The diagram in Figure 19 shows that the triaxial tests will fail with large cyclic shear strains for a range of average shear stresses about halfway between the compression and extension static shear strengths. For average shear stresses approaching the compression shear strength, the failure

mode will be dominated by large permanent compression shear strains, whereas for average shear stresses approaching the extension strength, the failure mode will be dominated by large permanent extension shear strains. Strains in compression are defined as positive and strains in extension are defined as negative in Figure 19 and later figures.

The intersection of the contours with the τ_a-axis and the location of the contours for values of τ_a approaching the static undrained shear strength depend upon the duration of τ_a. The reason is the undrained creep that occurs under high average shear stress. In the diagrams in this paper, the contours have been drawn to intersect the horizontal axis at the undrained shear strength in standard laboratory tests. If the duration of τ_a deviates from the approximately 2 h time to failure in standard monotonic laboratory test, this can be corrected for when applying the diagrams by using a shear strength corrected for load duration when denormalizing τ_a/s_u. The shear strength correction can be based on the data in Figure 20, which shows the shear strength of several clays as function of time to failure.

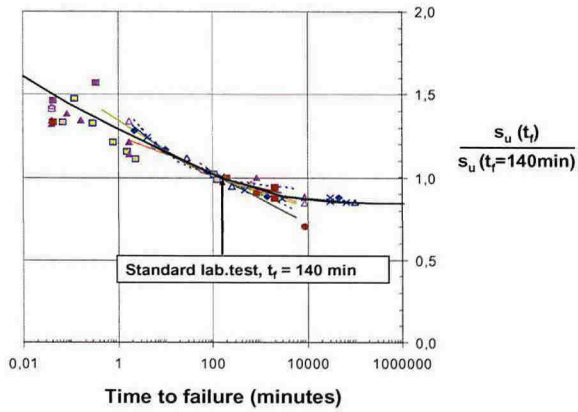

Figure 20. Static shear strength of several clays as function of time to failure (based on Lunne and Andersen, 2007).

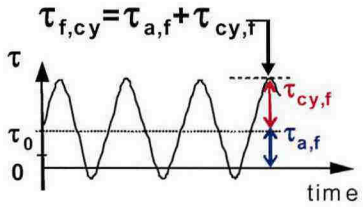

Figure 21. Definition of cyclic shear strength, $\tau_{f,cy}$.

Cyclic shear strength

The diagrams in Figures 18 and 19 show the combinations of average and cyclic shear stresses that will cause failure in a given number of cycles. In a stability analysis, one needs to know the maximum shear stress that can be mobilized. As illustrated in Figure 21, the maximum shear stress that can be mobilized is the sum of average and cyclic shear stresses at failure, i.e.

$$\tau_{f,cy} = \tau_{a,f} + \tau_{cy,f},$$

where: $\tau_{f,cy}$ is the cyclic shear strength, $\tau_{a,f}$ is the average shear stress at failure and $\tau_{cy,f}$ is the cyclic shear stress at failure.

$\tau_{a,f}$ is composed of the initial consolidation shear stress, τ_0, plus the change in average shear stress, $\Delta\tau_a$, due to an additional average load or redistribution of average stresses, i.e. $\tau_{a,f} = \tau_0 + \Delta\tau_a$. For clays, $\Delta\tau_a$ would normally be undrained, but for sands, $\Delta\tau_a$ may be drained.

The equation above means that the cyclic shear strength for a given number of cycles to failure can be established by simply adding average and cyclic shear stresses for various given values of average shear stress in the diagrams in Figures 18 and 19, and plot this sum as a function of the average shear stress. This is done as illustrated for DSS tests in Figure 22 and for triaxial tests in Figure 23. The reason for the discontinuity in the curves for triaxial tests in Figure 23 is that the average stress has opposite sign for compression and extension. Compression is defined as a failure mode where the permanent shear strain is positive, and extension is

defined as the failure mode where the permanent shear strain is negative.

The cyclic shear strength diagrams show that the cyclic shear strength can be higher than the static shear strength, as $\tau_{f,cy}/s_u>1$ for low number of cycles in some cases. This is because the clay strength is rate dependent (e.g. Figure 20). Since the cyclic tests are run with a load period of 10 s and the monotonic tests are brought to failure in about 2 h, the cyclic strength may thus be higher than the conventional static shear strength.

The diagrams in Figures 22 and 23 provide the data required to define the cyclic shear strength for the various stress conditions shown in Figure 15.

All the diagrams in this paper assume that $\Delta\tau_a$ is applied undrained. A diagram showing the effect of applying $\Delta\tau_a$ drained is presented for normally consolidated Drammen Clay in Andersen, 1988. The effect of drained versus undrained $\Delta\tau_a$ for very dense sand in presented in Andersen and Berre, 1999.

The diagrams also assume that the soil is undrained during a cycle. If it is possible for drainage or pore pressure redistribution to occur during a cycle, as it may be for sand in some cases, one should consider to limit the cyclic strength to the drained shear strength.

Equivalent number of cycles

The diagrams in Figures 22 and 23 give the cyclic shear strength for cases with a constant cyclic shear stress during the cyclic load history. In a storm, however, the cyclic shear stress is likely to vary from one cycle to the next. The equivalent number of cycles of the maximum cyclic shear stress, N_{eqv}, that would give the same effect as the real cyclic load history must therefore be determined in order to be able to use the diagrams.

Procedures to determine N_{eqv} are presented by Andersen (1976) and Andersen *et al.* (1992). The procedures use shear strain or pore pressure contour diagrams of the type presented in Figures 24 and 25. The diagrams are established from the same tests as used to establish the diagrams in Figures 18 and 19. The diagrams in Figures 24 and 25 are for DSS tests with an average shear stress of $\tau_a=0$. Similar diagrams can be established for other average shear stresses and for triaxial tests. Various such diagrams are given in Andersen (2004).

For undrained conditions, N_{eqv} can be determined by the "strain accumulation" procedure where the cyclic shear strain is used as memory of the cyclic effect by keeping track of the cyclic shear strain during the cyclic load history.

For sands or situations where drainage can occur during the storm, it is necessary to account for the effect of the drainage. The equivalent number of cycles, N_{eqv}, can then be determined by keeping track of the permanent pore pressure accumulated during the cyclic load history, accounting for the simultaneous generation and dissipation of the excess pore pressure. Andersen *et al.*, 1994 describes the pore pressure accumulation procedure and how the pore pressure dissipation can be taken into account.

In principle, the pore pressure accumulation procedure could also be used for clays. In practice, however, accurate laboratory measurement of pore pressure is more difficult to perform in clays than in sand. Since drainage is not likely to occur during the cyclic load history in clays, it may be preferable to use the cyclic strain accumulation procedure for clays.

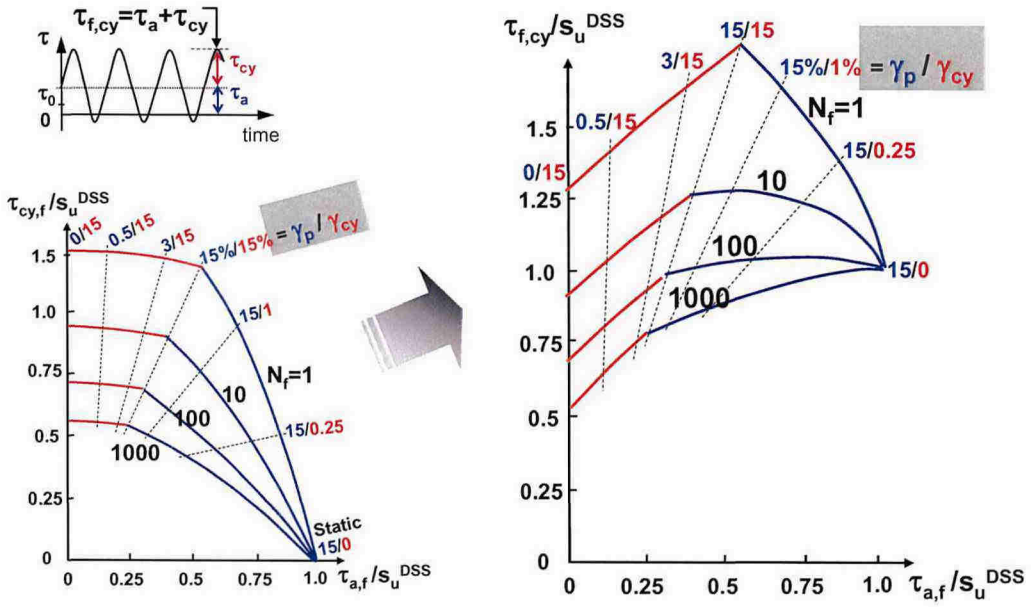

Figure 22. Cyclic DSS shear strength. Normally consolidated Drammen Clay.

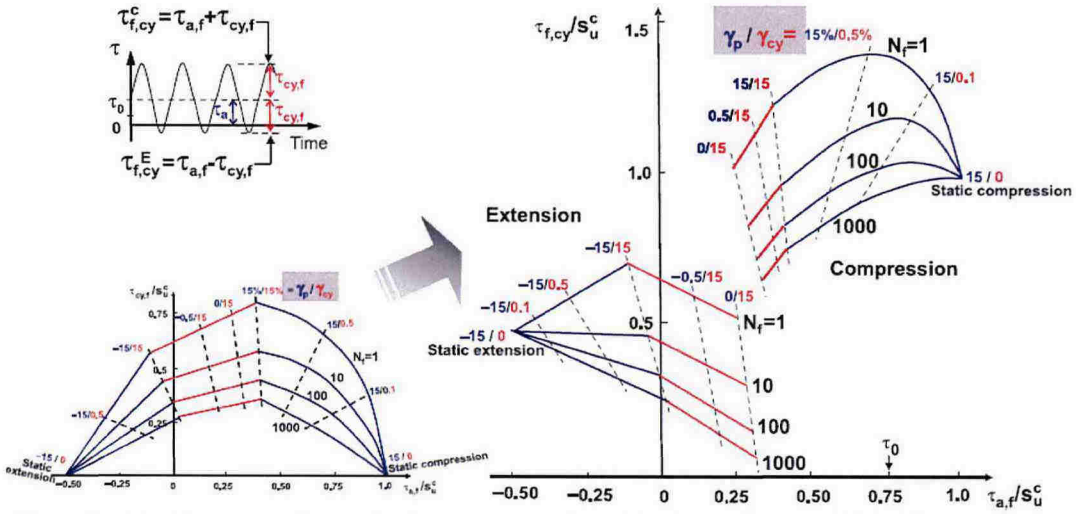

Figure 23. Cyclic triaxial compression and extension shear strengths. Normally consolidated Drammen Clay

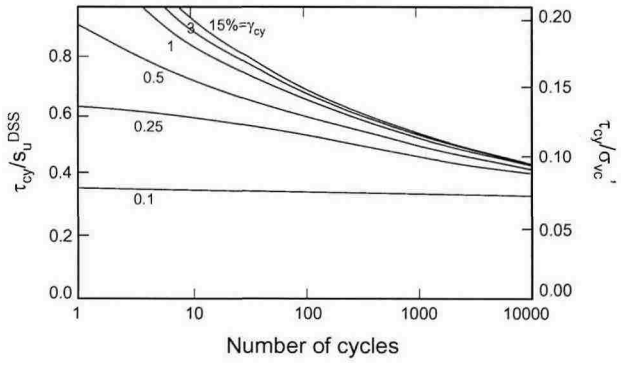

Figure 24. Cyclic shear strain as function of number of cycles (DSS tests with τ_a=0 on Drammen Clay with OCR=1). σ_{vc}' = vertical effective consolidation stress.

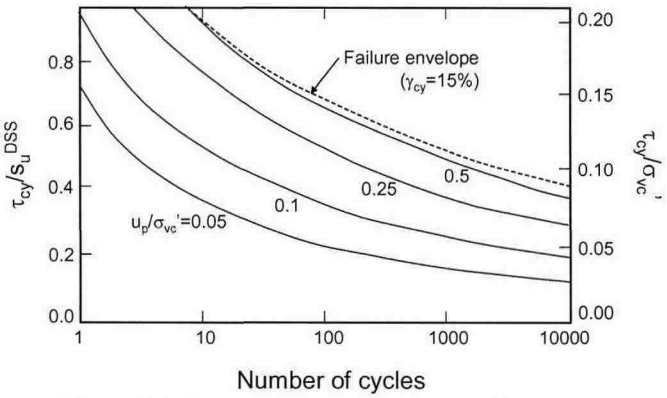

Figure 25. Permanent pore pressure as function of number of cycles (DSS tests with τ_a=0 on Drammen Clay.

CYCLIC STRENGTH DIAGRAMS FOR PRACTICAL APPLICATIONS

Importance of databases

Diagrams with cyclic shear strength of clay, silt and sand that have been established from DSS and triaxial laboratory tests are presented in this and the preceding sections. The data are compiled from NGI files and from the literature. The literature sources are included in the list of references at the end of the paper. The literature sources are Evans and Zhou, 1995, Finn, 1981, Hatanaka *et al.*, 1988, Hosono and Yoshimine, 2004, Hyde *et al.*, 2006, Hyodo *et al.*, 1994, Hyodo *et al.*, 1991, Hyodo *et al.*, 1996, Ishihara and Takatsu, 1979, Kokusho *et al.*, 2004, Koseki and Ohta, 2001, Koseki *et al.*, 2005, Lee and Seed, 1967, Lee and Vernese, 1978, Mulilis *et al.*, 1975, Mulilis *et al.*, 1977a, Mulilis *et al.*, 1977b, Oda *et al.*, 2001, Park and Byrne, 2004, Porcini *et al.*, 2004, Sakai and Ochai, 1986, Seed *et al.*, 1977, Siddiqi, 1984, Silver *et al.*, 1976, Sivathalayan and Ha, 2004, Tatsuoka *et al.*, 1986a, Tatsuoka *et al.*, 1986b, Tatsuoka *et al.*, 1988, Toki *et al.*, 1986, Tanaka *et al.*, 1987, Triantafyllidis *et al.*, 2004, Vaid and Chern, 1983, Vaid and Finn, 1979, Vaid *et al.*, 1999, Wijewickreme *et al.*, 2004, Wijewickreme and Sanin, 2005, Wong *et al.*, 1975, and Yoshimi *et al.*, 1994.

The diagrams can be used to determine parameters for feasibility studies before site-specific data are available. The diagrams can also be used as guides when specifying and interpreting site-specific cyclic laboratory tests. This will help to reduce the required number of site-specific cyclic tests and to evaluate their quality. Many of the diagrams presented in the following have already successfully served these purposes in practical projects.

For final design, the parameters from the diagrams should be verified by site specific laboratory tests.

Diagrams for normally consolidated Drammen Clay were presented in the preceding section. These diagrams have the format the diagrams ideally should have. Additional diagrams for clays are presented in the first part of this section. Thereafter, diagrams for sands and silts are presented. A database similar to the one for Drammen Clay is available for very dense clean Baskarp Sand (Andersen and Berre, 1999). Baskarp Sand is, however, more angular than most natural sands and may give strengths and moduli on the high side. The diagrams for silts and sands are less complete than for clay due to a lack of a general systematic testing programme similar to the ones on Drammen Clay and Baskarp Sand.

The main diagrams are for normally consolidated soils with moderate or no preshearing. The effect of over-consolidation and/or preshearing can be evaluated from additional diagrams that show the effect of these parameters.

All the diagrams in this paper are from stress-controlled cyclic tests with 10 s load period on non-cemented soils.

Cyclic shear strength of clays

Figures 18, 19, 22 and 23 present diagrams for normally consolidated Drammen Clay. The cyclic shear strength for a number of other normally consolidated clays are compared to Drammen Clay in Figures 26 and 27. There is a tendency for the normalized cyclic shear strength to increase with increasing plasticity index.

Diagrams for overconsolidated Drammen Clay with overconsolidation ratio of 4 and 40 can be found in Andersen (2004).

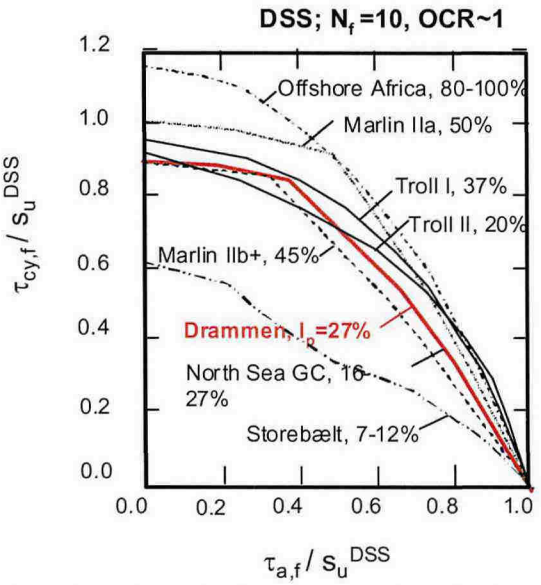

Figure 26. Normalized average and cyclic shear stresses for N_f=10 in DSS tests, for different normally consolidated clays (based on Andersen, 2004).

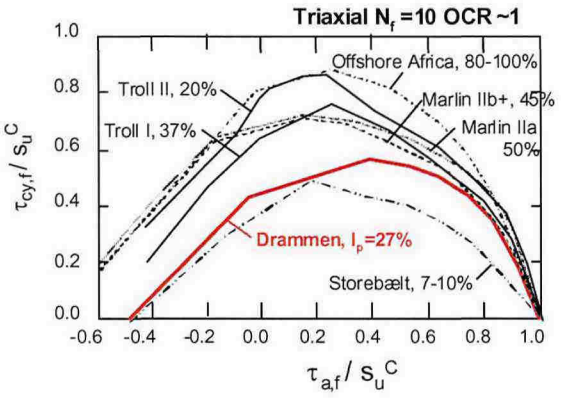

Figure 27. Normalized average and cyclic shear stresses for N_f=10 in triaxial tests, for different normally consolidated clays (based on Andersen, 2004).

CYCLIC SHEAR STRENGTH OF SANDS AND SILTS

Sample preparation

High quality samples of sands and silts that are representative of the in situ conditions are difficult to obtain. In cases where "intact" samples are very disturbed, one often reconstitutes the samples, but this may not give samples that are fully representative of the in situ conditions.

Silver *et al.*, 1976 and Mulilis *et al.*, 1977a have shown that the cyclic shear strength of sands and silts depends on the sample preparation method. Vaid *et al.* (1999) showed that water deposited sand closely simulated static and cyclic behaviour of frozen sand samples of natural alluvial and hydraulic fill. They also found that loose samples prepared by moist tamping gave weaker response than water deposited samples. Høeg *et al.* (2000) showed results for static shear strength of silty sand tailings with lower static strength for samples prepared by wet tamping than for "intact" samples at the same void ratio.

In several cases, however, samples prepared by wet tamping have given similar strength as "intact" samples. This is supported by Figure 28 which compares the cyclic triaxial shear strength of samples reconstituted by wet tamping with the strength of high quality frozen samples. A few results from water deposited and water vibrated samples do not deviate significantly from wet tamping and frozen samples. The tests on reconstituted samples are from various sources and thus not on the same soil as the frozen samples. The data in Figure 28 show that the samples reconstituted by wet tamping have similar cyclic shear strength as the frozen samples. These data thus indicate that wet tamping may give a reasonably realistic in situ cyclic shear strength. As shown later, wet tamping also seems to give similar cyclic shear strengths as "intact" samples (Figure 29), whereas dry tamping seems to give a tendency for lower strengths than wet tamping and "intact" samples (Figures 29 and 30).

Fines content more than a few percent will make reconstitution more difficult, especially if the fines also contain clay. Use of "intact" samples may then be possible and preferable, even if such specimens also will be disturbed. It is uncertain whether the disturbance may give too

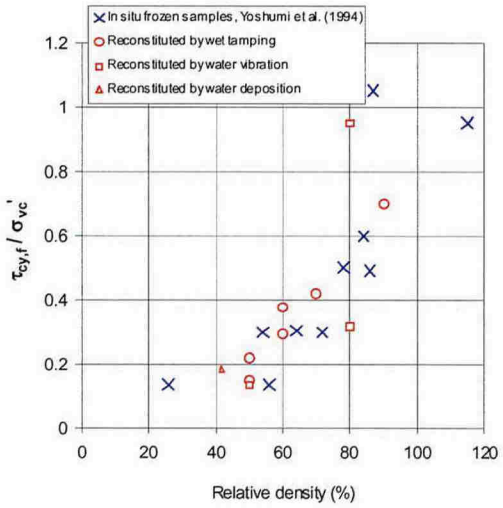

Figure 28. Cyclic shear stress to reach γ=3.75% after 10 cycles in isotropically consolidated triaxial tests on different sands as function of relative density. Comparison of in situ frozen samples and samples prepared by wet tamping, water deposition and water vibration.

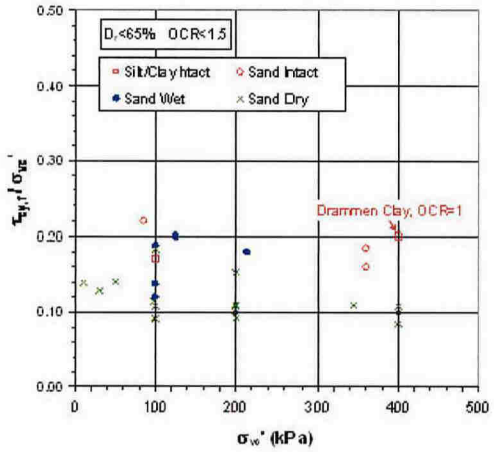

Figure 29. Shear strength for 10 cycles of symmetrical cyclic loading (τ_a=0) in DSS tests on different sands and silts with D_r<65% as function of vertical consolidation stress.

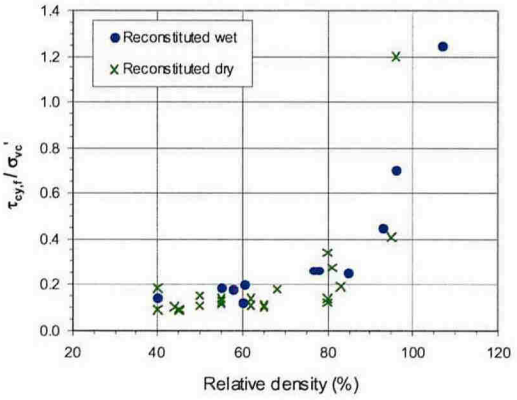

Figure 30. Shear strength for 10 cycles of symmetrical cyclic loading (τ_a=0) in DSS tests on different normally consolidated sands as function of relative density.

high or too low cyclic strength. This will depend on the relative density. If samples have to be reconstituted, they should be prepared wet, by tamping or water deposition, unless the in situ soil has been deposited under dry conditions.

The samples should be presheared if the soil is subjected to drained preshearing prior to and/or during the main design event. Herein, preshearing is meant cyclic loading accompanied by drainage during or after the cyclic loading. For large offshore gravity platforms on dense sand preshearing has typically been estimated to about 400 cycles at τ_{cy}/σ_{vc}'=0.04, as this has been estimated to occur during the build-up period of the design storm or during smaller storms prior to the design storm. In earthquake areas, the soil may have experienced smaller earthquakes during its history. Preshearing will increase the cyclic shear strength. Prehearing may also reduce the effect of the sample preparation method, but this has not been systematically studied.

Effect of consolidation time

There seems to be a long term effect of the consolidation time of reconstituted samples, even for clean sand. Tatsuoka *et al.* (1986a) found that the cyclic strength in isotropically consolidated triaxial tests on air pluviated Toyoura sand with no fines content increased by 15-20% after 68 days, for relative densities of both 50 and 80%. Tatsuoka *et al.* (1988) found that the cyclic shear strength of isotropically consolidated triaxial tests on water-vibrated Sengenyama Sand with 2.4% fines and D_r=80% increased by about 25% after 64 hours and 40% after 68 days. Mulilis *et al* (1977b) found that the cyclic strength of isotropically consolidated triaxial tests on air pluviated Monterey No. 0 sand with no fines at D_r=50% was essentially the same after 20 minutes and

one day consolidation, whereas it increased by 12% and 26% after 10 and 100 days consolidation time, respectively. The cyclic strength in DSS tests at NGI on air pluviated Oosterschelde Sand with no fines and D_r=62%, however, gave the same cyclic shear strength after 16 hours and 4 days consolidation.

For conventional projects it may be impractical to reproduce the long term effect in the laboratory, but the consolidation stress should act overnight for samples with some fines content. The effect of longer consolidation time must be evaluated by judgement and experience as referenced above. The experience above is from reconstituted samples with no preshearing, and one should be aware that the effect is likely to be less on intact samples and on samples with preshearing.

Cyclic shear strength in symmetrical DSS loading

The cyclic DSS shear strength for 10 load cycles of different normally consolidated sands prepared by wet and dry reconstitution is plotted in Figure 30.

The cyclic shear strength depends on the shear strain used to define failure, especially for densities above D_r=65%. Failure is defined as large shear strains of γ=7.5-15% for most of the points in Figure 30, but in a few cases failure is defined at a lower strain. This includes the data point for Baskarp Sand at τ_{cy}/σ_{vc}'=1.2, which is for γ=3% and which would plot even higher if a higher failure strain had been used.

The samples with D_r<85% in Figure 30 have been presheared with 400 cycles at τ_{cy}/σ_{vc}'=0.04 or less. The samples with $D_r \leq 85\%$ have been presheared with 400 cycles at τ_{cy}/σ_{vc}' between 0.075 and 0.1.

The plot in Figure 30 shows that the cyclic shear strength increases with relative density, especially for relative densities above D_r=65%. The cyclic shear strength is less dependent on relative density below D_r=65%. The plot in Figure 30 contains results from tests on both wet and dry reconstituted samples. The results from the tests on samples with dry reconstitution generally tend to plot lower than those with wet reconstitution. Based on the earlier discussion, one should disregard the results from reconstituted dry specimens.

Figure 30 contains data from tests with consolidation stresses in a range of σ_{vc}'=10 – 710 kPa. The cyclic shear strengths for relative densities D_r<65% was plotted in Figure 29 as function of consolidation stress to see what effect the consolidation stress may have. Figure 29 also contains data for normally consolidated Drammen Clay and some loose to medium dense silty soils that were not included in Figure 30 because of the problems of assessing relative density with silty soils. Some of these tests were run on "intact" samples. The samples in Figure 29 have been presheared with 400 cycles at τ_{cy}/σ_{vc}'=0.05 or less.

As seen earlier, the samples that were reconstituted dry tend to give the lowest cyclic shear strengths, and these are believed to underestimate the in situ shear strength. The "intact" samples and the samples reconstituted wet tend to give similar results. It is interesting to notice that the cyclic shear strength of normally consolidated Drammen Clay plot in the high range of the sand and silt data. There is a tendency for sand to have smaller cyclic shear strength than silt/clay, and the cyclic shear strengths are generally lower than the cyclic shear strength of Drammen Clay. This is in line

with the results for clays in Figures 26 and 27 which seem to indicate that the cyclic shear strength decreases with decreasing plasticity. Attempts to plot the cyclic shear strength of sand and silt as function of grain size or the grain size uniformity coefficient did not show any clear trend.

The data in Figure 29 show that there is some tendency for the normalized cyclic shear strength to increase with decreasing consolidation stress. This tendency may be more pronounced below σ_{vc}'=100kPa where there is no data for intact samples and samples prepared by wet reconstitution.

Dense soils (D_r>65%) may also deviate from the trend in Figure 29 and give a greater increase in strength ratio with decreasing $\tau_{cy,f}/\sigma_{vc}$'. For instance, DSS tests on air pluviated Fraser River sand with D_r~80% gave about 25% increase in $\tau_{cy,f}/\sigma_{vc}$' for σ_{vc}'=100 kPa compared to tests with σ_{vc}'=200 kPa. Tests with D_r~40-44% gave a smaller increase (about 10%) in $\tau_{cy,f}/\sigma_{vc}$' when decreasing σ_{vc}' from 200 to 100 kPa (Park and Byrne, 2004, Wijewickreme D. *et al.*, 2004).

Calcareous soils may also deviate from the trend in Figure 29. Experience from testing of calcareous silts and sands shows that calcareous soils tend to give similar or slightly higher normalized cyclic shear strength, $\tau_{cy,f}/\sigma_{vc}$', than the non-calcareous soils in Figure 29 at vertical consolidation stresses above 250 kPa. For lower consolidation stresses, however, laboratory tests have shown a significant increase in $\tau_{cy,f}/\sigma_{vc}$' with decreasing σ_{vc}' for calcareous soils. The tests on calcareous soils have generally been on intact samples from relatively shallow depth.

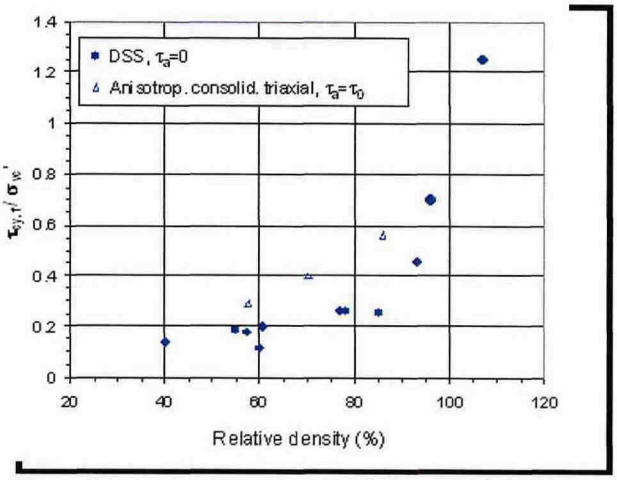

Figure 31. Cyclic shear stress to failure in 10 cycles in anisotropically consolidated triaxial tests with τ_a=τ_0 compared to DSS tests. Different normally consolidated sands prepared by wet tamping, as function of relative density. τ_0 is about 0.25σ_{vc}' to 0.275σ_{vc}'.

Reasons for the significant increase in $\tau_{cy,f}/\sigma_{vc}$' with decreasing σ_{vc}' may be that calcareous soil has high angularity, but may also be due to cementation or overconsolidation, even if they are not characterized as cemented or overconsolidated.

Cyclic strength in triaxial tests

The cyclic shear stress that will bring anisotropically consolidated triaxial samples to failure in 10 cycles is compared to DSS tests in Figure 31. There are only 3 triaxial tests. One should therefore be cautious about drawing general conclusions. However, the normalized cyclic shear stress to failure, $\tau_{cy,f}/\sigma_{vc}$', is about 75% higher for the triaxial tests with τ_a=τ_0 than for the DSS tests with τ_a=0.

Cyclic shear strength and water content

The cyclic shear stress that gives failure in 10 cycles in DSS tests with symmetrical cyclic loading is plotted as function of the water content in Figure 32. The samples prepared by dry reconstitution tend to give lowest cyclic shear strength, as in previous figures.

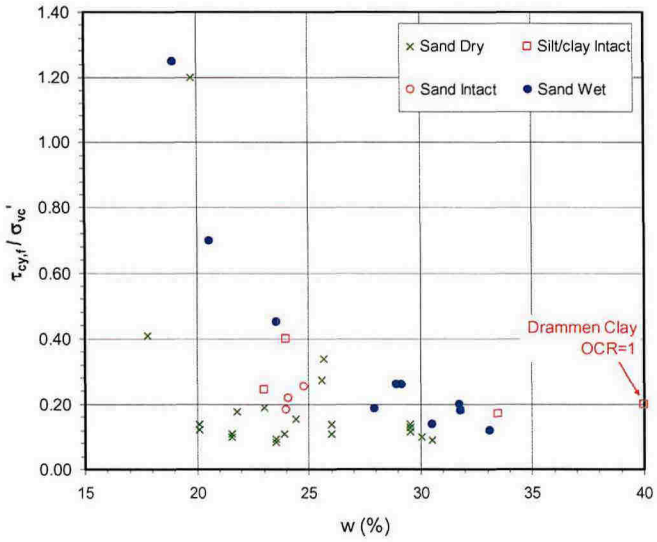

Figure 32. Shear strength for 10 cycles of symmetrical cyclic loading (τ_a=0) in DSS tests on different normally consolidated soils, as function of water content.

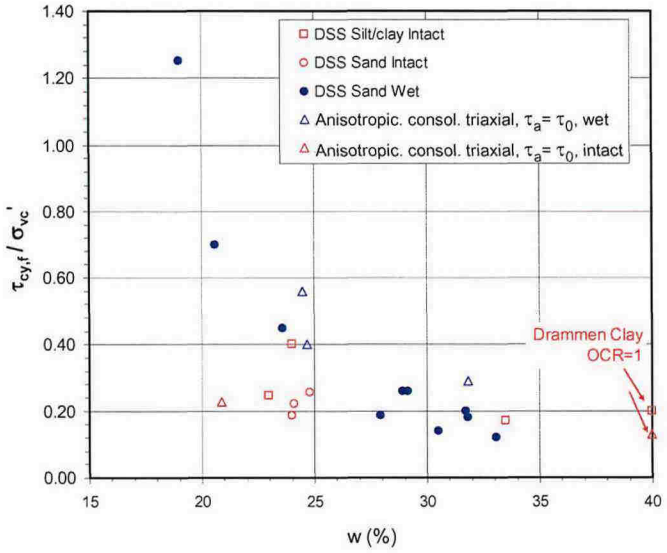

Figure 33. Cyclic shear stress to failure in 10 cycles in anisotropically consolidated triaxial tests with $\tau_a = \tau_0$ compared to DSS tests. Different normally consolidated sands prepared intact and by wet tamping, as function of relative density.

For the intact samples and the samples prepared by wet reconstitution, the normalized cyclic shear strength, $\tau_{cy,f}/\sigma_{vc}'$, increases with decreasing water content, especially as the water content decreases below a water content of about 25%. The effect of the water content is less significant above 25%.

Some of the scatter in $\tau_{cy,f}/\sigma_{vc}'$ below a water content of 25% is due to differences in consolidation stress, with a tendency for $\tau_{cy,f}/\sigma_{vc}'$ to increase with decreasing consolidation stress. The effect of consolidation stress was not large in the tests on sand with relative density below ~65% (Figure 29), but as mentioned before the effect of the consolidation stress may

be more pronounced at higher relative densities, i.e. at lower water content. Some scatter may also be due to uncertainty in the water content for some of the tests, as it was not clear in all the literature cases whether the reported water content was before or after consolidation. The water content after consolidation was used when it was available.

The cyclic shear stress that will bring anisotropically consolidated triaxial samples to failure in 10 cycles is compared to DSS tests in Figure 33. For the samples prepared by wet reconstitution, the normalized cyclic shear stress to failure, $\tau_{cy,f}/\sigma_{vc}'$, is higher in the triaxial tests with $\tau_a=\tau_0$ than in the DSS tests with $\tau_a=0$. This is the same tendency seen when $\tau_{cy,f}/\sigma_{vc}'$ was plotted as a function of relative density in Figure 31. The two triaxial tests on intact silt/clay samples show the opposite trend, but one should be cautious about drawing general conclusions with the limited number of triaxial tests available.

Effect of number of cycles

The cyclic shear stress that will bring DSS samples and anisotropically consolidated triaxial samples to failure for number of cycles different from 10 are plotted in Figures 34 and 35. The upper diagrams show the cyclic shear stress to failure normalized to the vertical effective consolidation stress, $\tau_{cy,f}/\sigma_{vc}'$. The lower diagrams show the cyclic shear stress to failure relative to the cyclic shear stress to failure in 10 cycles. The diagrams contain results from both intact samples and wet and dry sample preparation. Normally consolidated Drammen Clay is included for reference.

The data show that in DSS tests the cyclic shear stress to give failure in 3 cycles is about 20 to 40% higher than for 10 cycles. The difference between 3 and 10 cycles to failure shows more scatter for the triaxial tests. There are no systematic differences between intact samples and samples with wet and dry sample preparation. Drammen Clay tends to be somewhat less sensitivity to number of cycles to failure for DSS tests, but is closer to the average for triaxial tests.

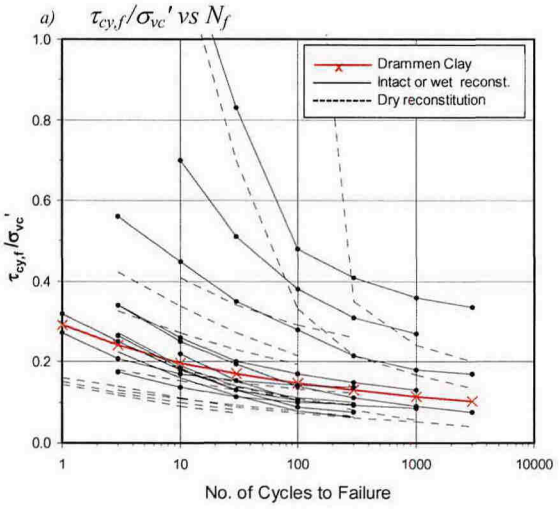

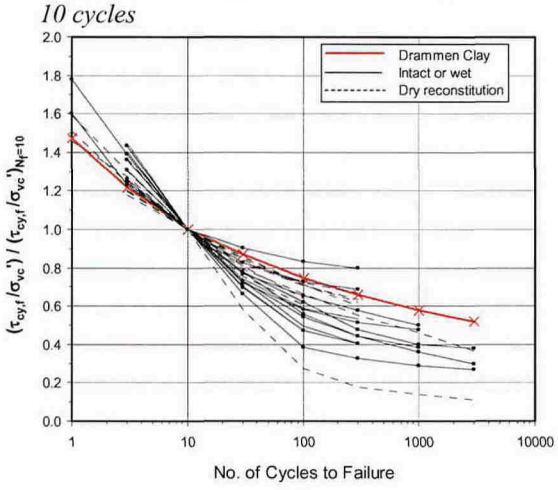

Figure 34. Cyclic shear stress to failure as function of number of cycles. DSS tests with symmetrical cyclic loading ($\tau_a=0$) on normally consolidated sands and silts. D_r-range 40-100%. Consolidation stress range 85-710 kPa.

The data in Figures 34 and 35 are for normally consolidated and close to normally consolidated soils. Less data are available for overconsolidated soils, but the data for a few overconsolidated soils indicate that they possibly follow the trend in Figures 34 and 35.

Effect of average shear stress

The diagrams in Figures 29-35 are for DSS tests with τ_a=0 and triaxial tests with τ_a=τ_0, where τ_0/σ_{vc}'~0.25-0.275. The cyclic shear strength is $\tau_{f,cy}$=$\tau_{a,f}$+$\tau_{cy,f}$, and the cyclic shear strength depends on the average shear stress. To fully define the cyclic shear strength, one therefore needs diagrams of the type presented for clays in Figures 18, 19, 26 and 27. Such diagrams are given for the very dense Baskarp Sand in Andersen and Berre (1999) for both undrained and drained $\Delta\tau_a$.

In triaxial tests with drained average shear stress, the cyclic shear strength will depend on the stress path for the average load, i.e. whether $\Delta\tau_a$ is applied by changing the vertical or the horizontal normal stress.

In dense soils that dilate under a change in average shear stress, the cyclic shear strength will generally be higher if $\Delta\tau_a$ is applied undrained than if it is applied drained. In soils that contract under a change in average shear stress, the cyclic shear strength may be lowest when $\Delta\tau_a$ is applied undrained.

Comparison between DSS and isotropically consolidated triaxial tests

The DSS test represents the best simulation of the in situ stress conditions for many situations. When DSS tests have not been available, isotropically consolidated triaxial tests have sometimes been used to estimate the cyclic shear

a) $\tau_{cy,f}/\sigma_{vc}$' vs N_f

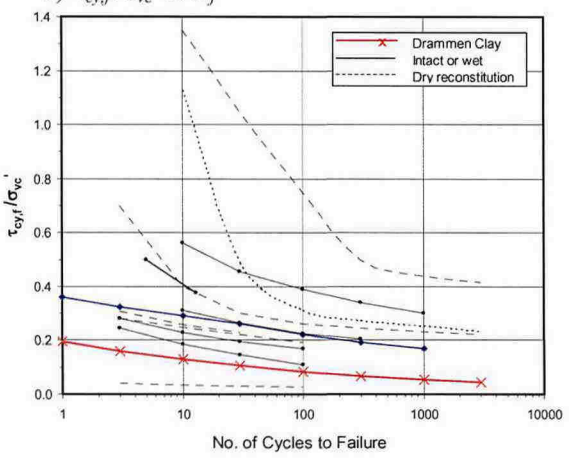

b) Normalized to cyclic shear stress to failure in 10 cycles

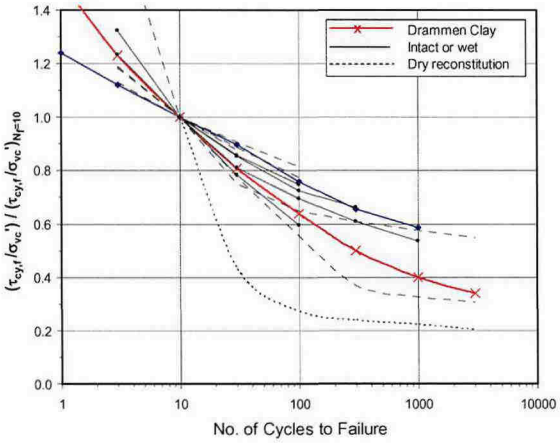

Figure 35. Cyclic shear stress to failure as function of number of cycles. Anisotropically consolidated triaxial tests with τ_a=τ_0=0.21-0.3·σ_{vc}' on normally consolidated sands and silts. D_r-range 35-96%. Consolidation stress range 100-710 kPa.

strength for DSS stress conditions, even if they do not model a representative stress path. Isotropically consolidated triaxial tests generally show higher cyclic shear stresses at failure, $\tau_{cy,f}/\sigma_{vc}$', than both the DSS and anisotropically consolidated triaxial tests when they are normalized to the vertical effective consolidation stress (Figure 36). To correct for this, one may assume that the strengths of DSS and isotropically consolidated triaxial tests will

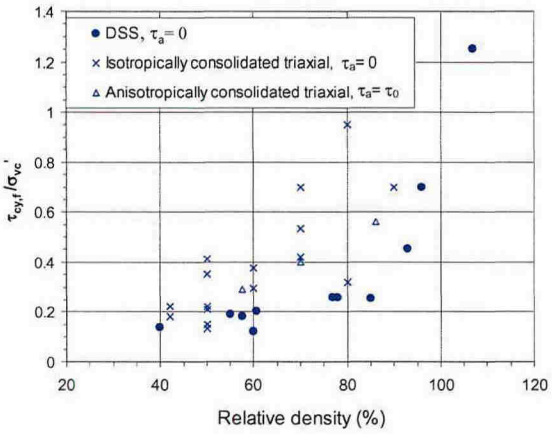

Figure 36. Cyclic shear stress to failure in 10 cycles in isotropically consoli-dated triaxial tests compared to triaxial tests with $\tau_a=\tau_0$ and DSS tests as function of D_r. Different normally consolidated sands prepared by wet tamping.

be the same when normalized to the octahedral effective consolidation stress. A comparison of available data show that normalization to the octahedral consolidation stress appears to give reasonable estimates of the cyclic DSS strength for D_r<65%. However, the horizontal consolidation stress needed to calculate the octahedral stress in the DSS test is uncertain. At higher relative densities, normalization to the octahedral consolidation stress seems to over-estimate the cyclic DSS strength.

One should generally be cautious about using isotropically consolidated triaxial tests, since the stress conditions in this test are normally not representative of the stress conditions beneath a structure.

Effect of preshearing

Sand deposits are often subjected to preshearing, i.e. small cyclic shear stresses accompanied by drainage, prior to the main design event, as discussed earlier. Preshearing may influence the undrained cyclic shear strength of a sand. Figure 37 shows how the undrained cyclic shear strength for 10 load cycles depends on the normalised cyclic shear stress, τ_{cy}/σ_{vc}', and the number of cycles during preshearing.

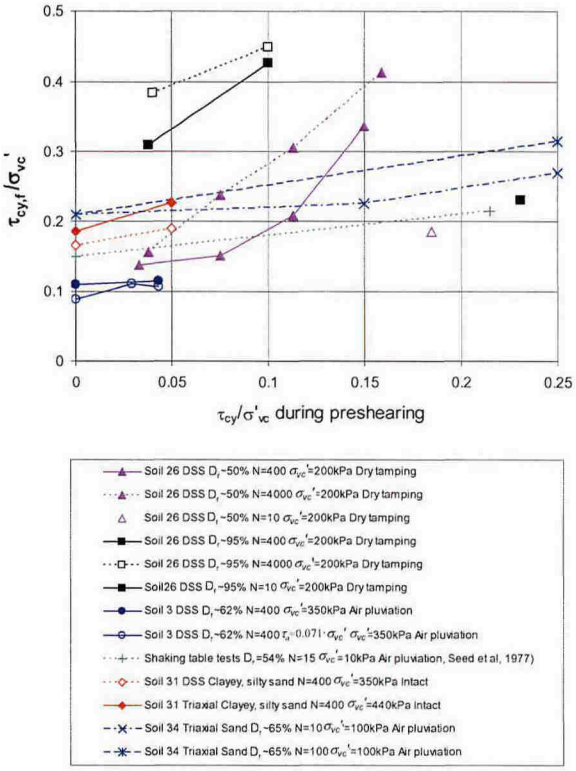

Figure 37. Effect of preshearing on undrained cyclic shear stress at failure in triaxial and DSS tests on sand/silt.

The figure contains DSS, shaking table and triaxial tests subjected to various degrees of preshearing.

In DSS tests, the preshearing may

- improve the seating between the sand and the horizontal end plates
- level out stress concentrations from the consolidation
- increase the horizontal effective stress
- change the soil structure

The volume reduction is generally small during preshearing, and the increase in density is by far not large enough to explain the increased cyclic resistance. One might expect preshearing to have less effect in triaxial tests than in DSS tests, since seating and stress concentrations are likely to be less important and the horizontal stress is kept constant in triaxial tests.

The data in Figure 37 show that

- the cyclic shear stress at failure increases with increasing preshearing, i.e. both with increasing cyclic shear stress and increasing number of cycles during preshearing
- preshearing has an important effect for both low and high relative density. No clear trend is observed as function of D_r.
- there are less data with preshearing in triaxial than in DSS tests, and the data do not show clear differences between triaxial and DSS tests
- preshearing with 400 cycles at τ_{cy}/σ_{vc}'=0.04 may give a cyclic shear strength increase between about 5 and 25%.

The effect of preshearing may be the opposite of what is presented above if the preshearing causes large shear strains that may break down the structure, e. g. Oda *et al* (2001) and Wijewickreme and Sanin (2005).

The data above are for normally consolidated soil. Preshearing may give less positive effect on overconsolidated soil. Cyclic tests on Drammen Clay show that preshearing at a cyclic shear stress of half the static shear strength gives an increased resistance to subsequent undrained cyclic loading in normally consolidated clay, but a reduced resistance in clay with an overconsolidation ratio of 4 (e.g. Andersen, 1988). Similar effects of overconsolidation may also exist for cohesionless soil, but no data have been available for overconsolidated sand.

Effect of overconsolidation

The in situ soil may be overconsolidated due to removal of previous overburden, variation in the weight of the structure, or preloading by temporary weight or underpressure. Overconsolidation will increase

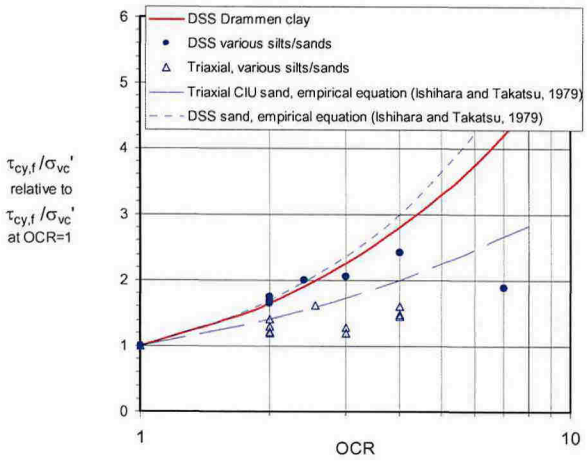

Figure 38. Effect of overconsolidation on cyclic shear stress at failure for 10 load cycles in DSS tests with symmetrical loading (τ_a=0) and in triaxial tests. CIU = isotropically consolidated triaxial test.

the horizontal effective normal stress, increase the relative density and possibly change the structure. These changes will tend to increase the cyclic resistance of the soil.

The effect of overconsolidation on the cyclic shear stress at failure, $\tau_{cy,f}/\sigma_{vc}'$, was compiled for different cohesionless soils in Figure 38. Both loose and dense soils are included. Drammen Clay and an empirical equation from Ishihara and Takatsu (1979) are included as references. The equation from Ishihara and Takatsu (1979) is applied for two conditions; (1) K_0-value of 0.5, 0.7, 1.0 and 1.35 for OCR= 1, 2, 4 and 8, respectively, and (2) K_0=1.0 for all overconsolidation ratios, OCR. The first condition simulates one-dimensional consolidation, like in the DSS test. The second condition represents isotropically consolidated triaxial conditions where K_0 does not change due to overconsolidation.

The data in Figure 38 show that:

- overconsolidation increases the resistance to cyclic loading significantly
- the effect of overconsolidation on the cyclic shear stress at failure is typically about 50% higher in DSS than in triaxial

tests. One reason for this is likely the increase in K_0 with OCR in the DSS tests. If the triaxial tests are run by adjusting K_0 as function of OCR, one would expect the same effect of OCR as in the DSS tests.

- the increase in the cyclic DSS strength for the non-cohesive soils is close to or slightly smaller than the increase measured on Drammen Clay.
- the empirical equations from Ishihara and Takatsu (1979) give a somewhat greater effect of overconsolidation than the data points, but also indicate a difference between DSS and isotropically consolidated triaxial tests.

Effect of load period

All results presented in this paper are from tests with 10 s load period. There is scatter in the data, but experience from testing of several offshore clays is that one 100 s load cycle has the same effect as 1.5 to 5 cycles with 10 s load period. The observation is for clays with plasticity index in the range of I_p=40-100%. There is not a clear trend, but the effect of a longer load period seems to be highest for tests with high plasticity index, I_p.

The tests on quick clay in the subsequent section show that one 10 s cycle seems to have the same effect as about eight 1 s cycles.

Cyclic tests on sand seem to indicate no significant effect of load period (Lee and Vernese, 1978, Tatsuoka *et al.*, 1986a). No systematic data has been found for silt, but it seems reasonable to expect an effect between the effect for clay and sand, depending on the silt, sand and clay content.

Cyclic data for displacement analyses

Data for calculation of cyclic displacements, equivalent soil stiffnesses for structural dynamic analyses, permanent displacements due to cyclically induced shear strains and dissipation of cyclically induced pore pressure are presented in Andersen (2004) for clay and in Andersen *et al.* (1994) and Andersen and Berre (1999) for sand.

The data are presented in the same format as for cyclic stresses to failure in Figures 18 and 19, but with contours of permanent and cyclic shear strains and permanent pore pressure for given number of cycles instead of contours of number of cycles to failure.

Procedures to calculate the different displacement components are proposed in Andersen (1991) and Andersen and Høeg (1991).

Capacity calculation

The capacity of a foundation under combined static and cyclic loading can be calculated by limiting equilibrium analyses with the procedure proposed by Andersen & Lauritzsen (1988). The cyclic shear strength of the clay is determined from diagrams such as in Figures 22 and 23. The cyclic shear strength at a given point on the failure surface (see Figure 15) is interpolated between the strengths from compression, DSS, and extension tests. The procedure accounts for the redistribution of average soil stresses during cyclic loading and determines whether the failure mode will be large cyclic displacements, large average displacements, or a combination of the two. The procedure is based on the assumption that the combination of average and cyclic shear strains is the same along the potential failure surface (strain compatibility), and on the condition that the average shear stresses along the potential failure surface is in equilibrium with the average loads.

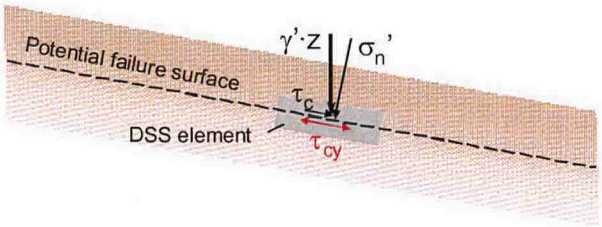

Figure 39. Simplified stress conditions in infinite slope.

The capacity of piles under vertical cyclic loading can be calculated by modelling the pile-soil interface with non-linear "t-z"-springs (Karlsrud and Nadim, 1990) where t and z represent mobilized skin friction and vertical displacement, respectively, with cyclic and permanent components determined through strain contour diagrams of the type mentioned in the section "Cyclic data for displacement analyses" above.

CLAY SLOPES UNDER EARTHQUAKE LOADING

Special considerations for quick clay and slopes subjected to earthquake

For slopes subjected to earthquake loading, the stress conditions and the failure mechanism require special considerations. A permanent slope will consolidate under a shear stress from its own weight, τ_c, as illustrated in Figure 39. For relatively steep slopes, this average shear stress may be of about the same magnitude as the cyclic shear stress due to the earthquake. The earthquake has a cyclic load period about one tenth of offshore wave loading.

This section presents preliminary results from an on-going laboratory testing programme where such conditions are modelled. The tests were run on high quality block samples of a Norwegian Quick Clay with a sensitivity of more than 75. The samples were normally consolidated with water content of about 39%, clay content of about 40%, plasticity index of about 10-12%, and an apparent overconsolidation ratio due to secondary consolidation less than 1.5. The preconsolidation stress was obtained from constant rate of strain oedometer tests.

Quick clay was used for the testing because new Norwegian regulations may require slopes to be checked for earthquake loading, and some slopes in Norway contain quick clay. There is little experience with the cyclic behaviour of quick clay, and it was believed that quick clay may be more vulnerable to cyclic loading than ordinary clays.

The purpose of the testing was (1) to check cyclic behaviour under the stress conditions in a slope and (2) to study if quick clay behaves different from ordinary clays.

Cyclic behaviour of quick clay vs ordinary clays

The behaviour of the quick clay under cyclic loading is compared to normally consolidated Drammen Clay in Figure 40. The data in Figure 40 are for DSS tests with symmetrical stress controlled 10s load cycles. The number of cycles to failure is slightly lower for the quick clay than for Drammen Clay. The relatively small difference may be explained by differences from one soil to another. In particular, the quick clay had somewhat smaller clay content (40%) than Drammen Clay (45-55%) and some over-consolidation (OCR~1.5). Experience has shown that the cyclic shear strength may decrease with decreasing plasticity (e. g. Figures 26 and 27) and increasing overconsolidation ratio. The data thus show that the quick clay tested seems to behave similar to other clays under cyclic loading.

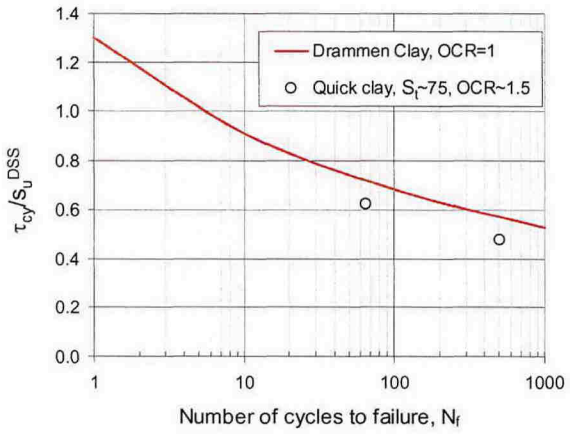

Figure 40. Number of cycles to failure for quick clay compared to Drammen Clay. DSS tests with symmetrical loading (τ_a=0) and 10 s load period. S_t = sensitivity.

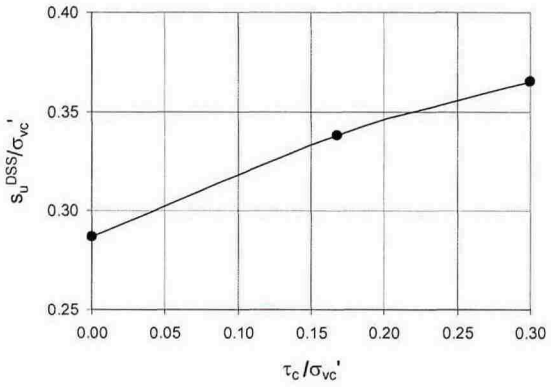

Figure 41. Undrained static DSS shear strength of the quick clay as function of normalized consolidation shear stress, τ_c/σ_{vc}'.

Effect of load period

The tests in Figure 40 are run with a load period of 10 s. Earthquakes have a period of about 1 s, and preliminary tests on the quick clay with different load periods indicate that the number of cycles to failure increases about 8 times when the load period is reduced from 10 to 1 s.

Effect of shear stress during consolidation

The undrained shear strength will increase if the clay is consolidated under a shear stress, as illustrated in Figure 41. The effect may be smaller in overconsolidated clay and may depend on plasticity.

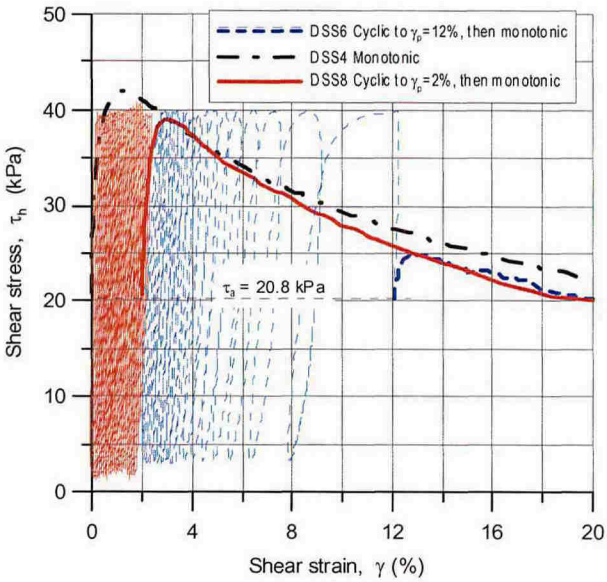

Figure 42. Stress-strain behaviour in monotonic, cyclic and post-cyclic monotonic DSS tests with $\tau_a=\tau_c$=20.8kPa = 0.16·σ_{vc}'. τ_h = horizontal shear stress.

The data in Figure 41 illustrates the importance of consolidating the clay under the appropriate stresses, both for monotonic and cyclic testing. If this strength increase is neglected, the stability of a slope under additional undrained loading may be significantly underestimated. On the other hand, a laboratory test is normally run to failure in less than 2 hours, and the slope will remain undrained for a much longer period than this after additional loading. The undrained shear strength may then be reduced by about 20%, according to Figure 20. Monotonic tests on the quick clay sheared with different strain rates agree well with the diagram in Figure 20.

Effect of cyclic loading on static shear strength

A series of tests were performed to see the effect of cyclic loading on the static shear strength of a slope. Examples of cyclic tests consolidated with τ_c/σ_{vc}'=0.16, corresponding to a slope of about 10^0, are presented in Figure 42. The figure shows one reference monotonic test and 2 cyclic

tests that were run with monotonic loading to failure after cycling. The monotonic tests were run strain-controlled with a rate of shear strain of ~4.5%/hr.

The reason why the cyclic stress-strain curves go beyond the monotonic stress-strain curve is that the cyclic tests are run stress-controlled and that the rate of strain is significantly higher in the cyclic tests when they develop large strains than the rate of strain in the monotonic tests.

The cyclic loading was stopped when a permanent shear strain of γ_p=2% was reached in the first cyclic test (DSS8) and when γ_p=12% was reached in the other cyclic test (DSS6). The results in Figure 42 show that the monotonic peak shear strength is reduced by the cyclic loading and that the post-cyclic monotonic stress-strain curves rapidly join the virgin monotonic stress-strain curve. Differences in the monotonic curves are believed to be due to soil variability. Series of tests consolidated under other shear stresses show better agreement. It thus appears that the post cyclic static shear strength is governed by the virgin monotonic stress-strain curve and the permanent shear strain that is developed during cyclic loading. Similar results have been found on Drammen Clay (Andersen, 1988), but the behaviour is even more evident for the quick clay due to the more pronounced strain-softening.

Tests with symmetrical cyclic loading (τ_a=τ_c=0) show a somewhat different picture, where the post cyclic monotonic stress-strain curve does not reach the monotonic stress-strain curve. This more severe effect of cyclic loading was seen both in tests on quick clay and Drammen Clay (Andersen, 1988).

Effect of cyclic loading on undrained creep

A slope subjected to an earthquake will experience both cyclic and permanent shear strains and displacements. However, the failure mode is not likely to be large cyclic shear strains and displacements because of the relatively significant average shear stress in a slope. The cyclic loading will instead cause large permanent shear strains and displacements, as in the tests in Figure 42. The failure is not likely to occur during the peak load either, because the duration of the peak load is not long enough to accelerate the soil mass. The critical mechanism is therefore likely to be development of large permanent shear strains and displacements during or after the earthquake. The critical period may be some time after the earthquake before the excess pore pressure generated by the cyclic loading has dissipated. During this period the clay will creep under undrained conditions and a delayed failure may occur. This is simulated in the DSS tests and illustrated by an example in Figure 43.

The test in Figure 43 has been consolidated with an average shear stress of 62% of the undrained static shear strength, corresponding to a slope of about 13^0. The specimen was cycled to a permanent shear strain of 5% and left with the average shear stress under undrained conditions. It can be seen that the specimen develops shear strains that accelerate and fails after 136 minutes.

A reference test is included in Figure 43 to verify that the test was not unstable after consolidation and that the creep failure was induced by the cyclic loading. The reference test was run by just closing the drainage after the same consolidation period as in the cyclic test. The reference test did not develop noticeable shear strains.

The failure mode for a slope subjected to earthquake loading is thus expected to be delayed undrained creep. Based on the results produced so far, the slope may be analysed by first running a dynamic analysis to determine the permanent shear strain due to the design earthquake. The post-cyclic shear strength may then be determined as the shear stress on the monotonic stress-strain curve at a shear strain equal to the calculated permanent shear strain. This shear strength should be reduced by 15-25% to account for (1) the post-cyclic stress-strain curve reaching the virgin curve at a somewhat larger strain than the permanent strain developed during the earthquake, and (2) the time to failure being significantly longer than in the monotonic laboratory test (see Figure 20).

In a quick clay slope there will be progressive failure mechanisms (e.g. Andresen and Jostad, 2004), and this must be taken into consideration when applying the shear strength discussed above.

VERIFICATION OF CALCULATED FOUNDATION CAPACITY BY MEANS OF MODEL TESTS

The use of laboratory test data, as presented above, to calculate the foundation capacity of structures subjected to cyclic loading was verified by predicting or back-calculating various series of model tests. The calculation method is briefly described earlier in the paper.

The model tests included:

- Five 1g laboratory model tests of an offshore gravity base structure with monotonic and cyclic loading on a soft clay (Andersen *et al.* 1989).
- Twelve 1g laboratory model tests with monotonic and cyclic loading on an offshore tripod gravity platform (Aas & Andersen 1992).

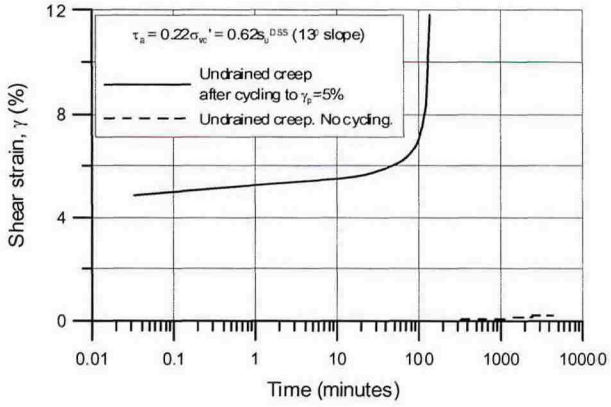

Figure 43. Development of shear strain in undrained DSS tests with constant shear stress.

- One monotonic and one cyclic centrifuge test of a gravity base structure similar to the Ekofisk Oil Storage Tank (Andersen *et al.*, 1994)
- Two series of large scale field tests with monotonic and cyclic loading of offshore suction anchors in clays. One series of tests was run with a load inclination of 10° with the vertical to simulate anchors for a tension leg platform (TLP) (Andersen *et al.* 1993 and Dyvik *et al*, 1993). The other series was run with a load inclination of 10° with the horizontal to simulate anchors *with* more horizontal loading (Keaveny *et al.* 1994).

The comparison of calculated and measured capacities are presented in the references for the various model tests above. The calculated bearing capacity, type of failure surface, failure surface location, and failure mode (large permanent displacements, large cyclic displacements, or a combination) agreed well with the measurements for all the model tests.

As an example, some details are given for the last of the model test series referenced above. The model geometry and the soil conditions are summarized in Figure 44. The model after it was brought to failure is shown in Figure 45.

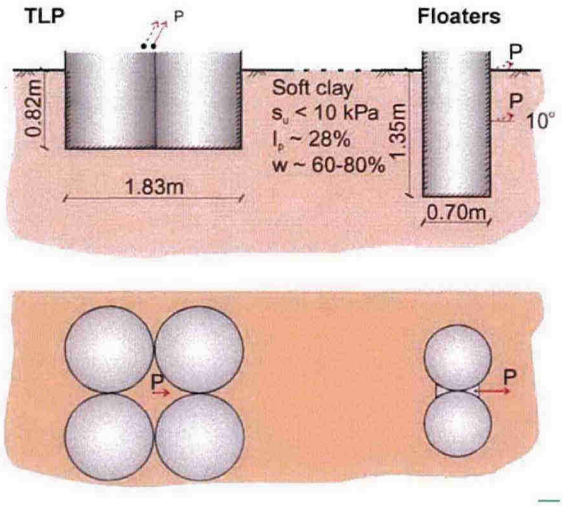

Figure 44. Geometry and key soil data for the large scale field model tests of offshore suction anchors. P = applied load.

Figure 45. TLP model after failure (photo by Rune Dyvik, NGI).

Table 1. Predicted and measured failure loads for the TLP field model tests

Test nr	Test type	Predicted /measured failure load
1	Monotonic	1.00
2	Cyclic	1.05
3	Cyclic	1.06
4	Cyclic	1.01

Predicted and measured capacities of the monotonic and the 3 cyclic TLP tests are compared in Table 1. The agreement is very good.

The predicted and observed failure surfaces are shown in Figure 46. This agreement is also generally good, but there are some differences. However, back-calculations with the observed failure surfaces

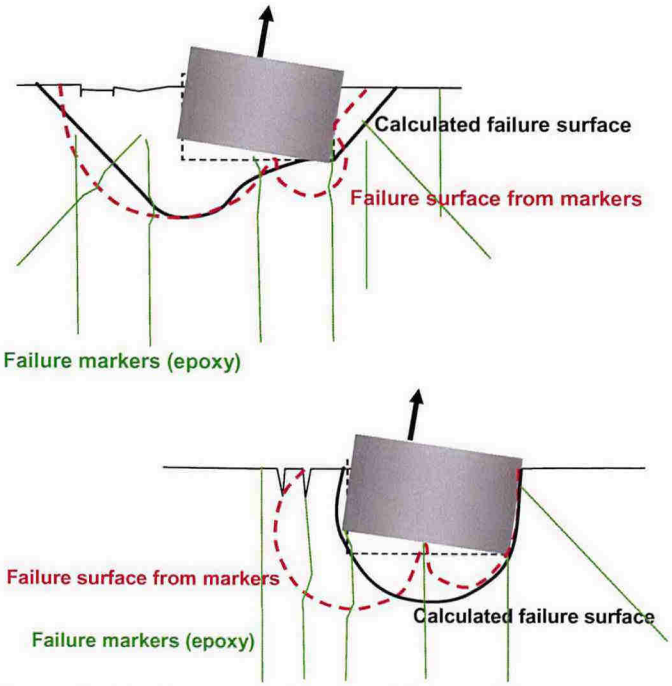

Figure 46. Predicted and observed failure surfaces in TLP model tests. Top: Tests 1, 2 and 3. Bottom: Test 4.

gave insignificant differences in the calculated capacities. The reason for the difference in failure surface between Test 4 and the other tests is that Test 4 was subjected to a greater moment.

SUMMARY AND CONCLUSIONS

Cyclic loading can be very significant for the foundation design of structures, both offshore, along the coast and on land, and for the stability of slopes.

The soil elements beneath a structure subjected to cyclic loading follow different stress paths. The behaviour under cyclic loading depends strongly on the stress path, and it is important to determine the cyclic shear strength under representative stress conditions. In practice, this can be done by DSS and triaxial tests consolidated to the appropriate in situ stresses prior to cyclic loading and run under representative combinations of average and cyclic shear stresses.

A convenient way to present the results from the cyclic tests is to prepare diagrams where the number of cycles to failure is plotted as a function of average and cyclic shear stresses. These diagrams should also contain the failure mode, i.e. the combination of permanent and cyclic shear strains at failure. The diagrams will thus contain the information that is required to calculate the capacity of a structure under cyclic loading by a limiting equilibrium method that accounts for (1) strain compatibility and (2) equilibrium between the weight of the structure and the average shear stresses in the soil.

The paper presents diagrams with cyclic shear strength of clay, sand and silt that can be used for practical design. These diagrams are useful for feasibility studies before site-specific cyclic data become available, and as guide when specifying and interpreting site-specific cyclic laboratory tests.

Some cases, like slopes under earthquake loading, may require special considerations, and the paper presents some data on cyclic testing of a quick clay under such conditions. One possible failure mode for this case is undrained creep initiated by the earthquake. The post-cyclic monotonic shear strength may also be reduced by the earthquake loading, making the slope vulnerable to increased loads or erosion in the period before the earthquake-induced excess pore pressures have dissipated.

Comparison between calculations and model tests indicate that foundation capacity under cyclic loading can be reliably determined on the basis of cyclic shear strength determined in laboratory tests.

ACKNOWLEDGEMENTS

The results presented in this paper are based on information from joint industry sponsored research projects, research projects funded by the Research Council of Norway, and consulting projects. Numerous colleagues at NGI have contributed to the results, both in performing and interpreting laboratory tests and model tests and by developing theoretical models. This co-operation is greatly appreciated. Special thanks are extended to Dr. Fritz Nowacki, NGI, for fruitful discussions through many years and projects, Mr. Jan Lampe, NGI, for his high quality and careful DSS testing, Dr. Amir Kaynia, NGI, for discussions on slope behaviour under earthquake loading, and Dr. Suzanne Lacasse, NGI, for reviewing and commenting on the paper.

REFERENCES

Aas, P.M. and Andersen, K.H. 1992. Skirted foundations for offshore structures. *In* Proceedings of the 9th Conference and Exhibition Offshore South East Asia.

Andersen, K.H. 1976. Behaviour of clay subjected to undrained cyclic loading. *In* Proceedings of the International Conference on the Behaviour of Offshore Structures, BOSS'76. Trondheim 1976. Vol. 1, pp. 392-403.

Andersen, K.H. 1988. Properties of soft clay under static and cyclic loading. *In* Proceedings of the Intern. Conf. on Eng. Problems of Regional Soils. pp. 7-26, Beijing, China, 1988. *Ed. by* Chinese Institution of Soil Mech. and Found. Engrg. *Also* publ. in NGI Publ. 176.

Andersen, K.H., Kleven, A. and Heien, D. 1988. Cyclic soil data for design of gravity structures. ASCE, J. Geotech. Engrg, **114**(5): 517-539.

Andersen, K.H. and Lauritzsen, R. 1988. Bearing capacity for foundation with cyclic loads. ASCE, J. Geotech. Engrg, **114**(GT5): 540-555.

Andersen, K.H., Dyvik, R., Lauritzsen, R., Heien, D., Hårvik, L. and Amundsen, T. 1989. Model tests of offshore platforms. II. Interpretation. ASCE, J. Geotech. Engrg, **115**(11): 1550-1568.

Andersen, K.H. 1991. Foundation design of offshore gravity structures. *In* Cyclic Loading of Soils. From Theory to Design. Chapter 4. *Ed. by* M.P. O'Reilly and S.F. Brown. *Publ. by* Blackie and Son Ltd., Glasgow and London. *Also:* NGI Publ. 185.

Andersen, K.H. and Høeg, K. 1991. Deformations of soils and displacements of structures subjected to combined static and cyclic loads. *In* Proceedings of the X ECSMFE, Firenze, May 1991, Vol 4, pp. 1147-1158.

Andersen K.H., Hansteen, O.E. and Gutierrez, M. 1991. Bearing capacity, displacements, stiffness and hysteretic damping of Storebælt bridge piers under ice loading. *In* Proceedings of the Seminar on Design of Exposed Bridge Piers. Danish Society of Hydraulic Engineering. Copenhagen, Denmark, 22 January 1991. *Also* published in NGI Publ. 199.

Andersen K.H., Dyvik, R., Kikuchi, Y. and Skomedal, E. 1992. Clay behaviour under irregular cyclic loading. *In* Proceedings of the Intern. Conf. on the Behaviour of Offshore Structures, London, Vol. 2., pp. 937-950.

Andersen, K. H., Dyvik, R., Schroder, K., Hansteen, O. E. and Bysveen, S. 1993. Field tests of anchors in clay. II: Predictions and interpretation. ASCE, J. Geotech. Engrg. **119**(10): 1532-1549.

Andersen, K.H., Allard, M.A. and Hermstad, J. 1994. Centrifuge model tests of a gravity platform on very dense sand; II: Interpretation. *In* Proceedings of the 7th Intern. Conf. on Behavior of Offshore Structures. BOSS'94. Cambridge, Mass. Vol. 1, pp 255-282.

Andersen K.H. and Berre, T. 1999. Behaviour of a dense sand under monotonic and cyclic loading. *In* Proceedings of the 12th ECSMGE, Geotech. Engrg. for Transp. Infrastructure., Amsterdam, The Netherlands. Vol.2, p. 667-676. *Publ. by* A.A. Balkema.

Andersen, K.H. 2004. Cyclic clay data for foundation design of structures subjected to wave loading. *In* Proceedings of the Intern. Conf. on Cyclic Behaviour of Soils and Liquefaction Phenomena, CBS04, Bochum, Germany, 31.3-2.4, 2004, p. 371-387, A.A. Balkema Publishers, *Ed. by* Th. Triantafyllidis.

Andersen, K.H., Murff, J.D., Randolph, M.F., Clukey, E., Erbrich, C., Jostad, H.P. Hansen, B. Aubeny, C., Sharma, P. and Supachawarote, C. 2005. Suction anchors for deepwater applications. *In* Proceedings of the ISFOG, Intern. Symp. on Frontiers in Offshore Geotechniques. 19-21 September, 2005. Perth, Western Australia, pp. 1-30.

Andresen, L. and Jostad, H.P. 2004. Analyses of progressive failure in long natural slopes. *In* Proceedings of NUMOG IX, *Ed.* by Pande & Pietruszczak . Taylor and Francis Group, London, p. 603.

Bjerrum, L. 1973. Geotechnical problems involved in foundations in the North Sea. Geotechnique **23**(3): 319-358.

Christophersen, H.P., Bysveen, S. and Støve, O.J. 1992. Innovative foundation design systems selected for the Snorre field development. *In* Proceedings of VI Intern. Conf. on Behaviour of Offshore Structures, 7-10 July 1992, Imperial College, London, pp. 82-94.

Clausen, C.J.F., DiBiagio, E., Duncan, J.M. and Andersen, K.H. 1975. Observed behaviour of the Ekofisk oil storage tank foundation. *In* Proceedings of the 7th Offshore Technology Conference, Houston 1975, Vol. 3, pp. 399-413.

Dyvik, R., Andersen, K.H., Hansen, S.B. and Christophersen, H.P. 1993. Field tests of anchors in clay. I: description. ASCE, Journal of Geotechnical Engineering. 119 (19): 1515-1531.

Evans, M. D. and Zhou, S. 1995. Liquefaction behaviour of sand-gravel composites. ASCE J. Geotech. Engrg., **121**(3): 287-299.

Finn, W.D.L. 1981. Liquefaction potential: Developments since 1976. *In* Proceedings of the Intern. Conf. on Recent Advances in Geotech. Earthquake Engrg. and Soil Dynamics. St. Louis, Mo., 1981, Vol. 2, pp. 655-681.

Hatanaka, M., Suzuki, Y., Kawasaki, T. and Endo, M. 1988. Cyclic undrained shear properties of high quality undisturbed Tokyo gravel. Soils and Foundations **28**(4): 57-68.

Hosono, Y. and Yoshimine, M. 2004. Liquefaction of sand in simple shear condition. *In* Proceedings of the Intern. Conf. on Cyclic Behaviour of Soils and Liquefaction Phenomena, CBS04, Bochum, Germany, 31.3-2.4, 2004. pp. 207-214, A.A. Balkema Publishers, *Ed. by* Th. Triantafyllidis.

Hyde, A.F.L, Higuchi, T. and Yasuhara, K. 2006. Liquefaction, cyclic mobility and failure of silt. ASCE, J. Geotech. Engrg, **132**(6): 716-735.

Hyodo, M., Murata, H., Yasufuku, N. and Fujii, T. 1991. Undrained cyclic shear strength and residual strain of saturated sand by cyclic triaxial tests. Soils and Foundations, **31**(3): 60-76.

Hyodo, M., Tanimizu, H., Yasufuku, N. and Murata, H. 1994. Undrained cyclic and monotonic triaxial behaviour of saturated loose sand. Soils and Foundations, **34**(1): 19-34.

Hyodo, M., Aramaki, N., Itoh, M. and Hyde, A.F.L. 1996. Cyclic strength and deformation of crushable carbonate sand. Soil Dyn. and Earthquake Engrg., 15: 331-336.

Høeg, K., Dyvik, R. and Sandbækken, G. 2000. Strength of undisturbed versus reconstituted silt and silty sand specimens. ASCE, J. Geotech. and Geoenv. Engrg. **126**(7): 606-617.

Ishihara, K. and Takatsu, H. 1979. Effects of overconsolidation and K_0 conditions on the liquefaction characteristics of sands. Soils and Foundations **19**(4): 59-68.

Karlsrud, K. and Nadim, F. 1990. Axial capacity of offshore piles in clay. *In* Proceedings of the 22nd OTC, Houston, Paper 6245, pp. 404-416.

Keaveny, J.M., Hansen, S.B., Madshus, C. and Dyvik, R. 1994. Horizontal capacity of large scale model anchors. *In* Proceedings of the XIII ICSMFE. New Delhi 1994. Vol. 2, pp. 677-680.

Kokusho, T., Hara, T. and Hiraoka, R. (2004). Undrained shear strength of granular soils with different particle gradation. ASCE J. Geotech. and Geoenv. Engrg., **130**(6): 621-629.

Koseki, J. and Ohta, A. 2001. Effects of different consolidation conditions on liquefaction resistance and small strain quasi-elastic deformation properties of sands containing fines. Soils and Foundations, **41**(6): 53-62.

Koseki, J., Yoshida, T. and Takeshi, S. 2005. Liquefaction properties of Toyoura sand in cyclic torsional shear tests under low confining stress. Soils and Foundations, **45**(5): 103-113.

Lee, K. and Seed, H.B. 1967. Dynamic strength of anisotropically consolidated sand. ASCE, J. Geotech. Engrg., **93**(5): 169-190.

Lee, K. and Vernese, F.J. 1978. End restraint effects on cyclic triaxial strength of sand. ASCE. J. Geotech. Engrg., **104**(6): 705-719.

Lunne, T. and Andersen, K.H. 2007. Soft clay shear strength parameters for deepwater geotechnical design. *In* Proceedings of the 6th Intern. Offshore Site Invest. and Geotech. Conf.; Confronting New Challenges and Sharing Knowledge, p. 151-176, 11-13 Sept. 2007, London, UK.

Mulilis, J.P., Chan, C.K., and Seed, H.B. 1975. The effects of method of sample preparation on the cyclic stress-strain behavior of sands. Rep. No. EERC 75-18. College of Engrg., Univ. of California, Berkeley, July, 1975.

Mulilis, J.P., Seed, H.B., Chan, C.K., Mitchell, J.K. and Arulanandan, K. 1977a. Effects of sample preparation on sand liquefaction. ASCE, J. Geotech. Engrg. **103**(2): 91-108.

Mulilis, J.P., Mori, K., Seed, H.B. and Chan, C.K. 1977b. Resistance to liquefaction due to sustained pressure. ASCE, J. Geotech. Engrg., **103**(7): 793-797.

Oda, M., Kawamoto, K., Suzuki, K., Fujimori, H. and Sato, M. 2001. Microstruct. interpret. on reliquefaction of saturated granular soils under cyclic loading. ASCE J. Geotech. and Geoenv. Engrg. **127**(5): 416-423.

Park, S.S. and Byrne, P.M. 2004. Numerical modeling of soil liquefaction at slope site. In Proceedings of the Intern. Conf. on Cyclic Behaviour of Soils and Liquefaction Phenomena, CBS04, Bochum, Germany, 2004, pp. 571-580, A.A. Balkema Publishers, *Ed. by* Th. Triantafyllidis.

Porcini, D., Cicciu, G. and Ghionna, V.N. 2004. Laboratory investigation of the undrained cyclic behaviour of a natural coarse sand from unditurbed and reconstituted samples. In Proceedings of the Intern. Conf. on Cyclic Behaviour of Soils and Liquefaction Phenomena, CBS04, Bochum, Germany, 2004, pp. 187-192, A.A. Balkema Publishers, *Ed by* Th. Triantafyllidis.

Sakai and Ochai 1986. Effects of initial static shear stresses on the liquefaction of sand. Memoirs of Faculty of Engineering, Kyushu University, Vol. 46, No. 1, March 1986.

Seed, H.B., Mori, K. and Chan, K.C. 1977. Influence of seismic history on liquefaction of sands. ASCE, J. Geotech. Engrg., **103**(4): 257-270.

Siddiqi, F.H. 1984. Strength evaluation of cohesionless soils with oversized particles. PhD dissertation, University of California, Davis, Calif.

Silver, M.L., Chan, C.K., Ladd, R.S., Lee, K.L., Tiedemann, D.A., Townsend, F.C.,

Valera, J.E. and Wilson, J.H. 1976. Cyclic triaxial strength of standard test sand. ASCE, J. Geotech. Eng., **102**(5): 511-524.

Sivathalayan, S. and Ha, D. 2004. Effect of initial stress state on the cyclic simple shear behaviour of sands. *In* Proceedings of the Intern. Conf. on Cyclic Behaviour of Soils and Liquefaction Phenomena, CBS04, Bochum, Germany, 2004, pp. 207-214, A.A. Balkema Publishers, *Ed by* Th. Triantafyllidis.

Tatsuoka, F., Toki, S., Miura, S., Kato, H., Okamoto, M., Yamada, S., Yasuda, S. and Tanizawa, F. 1986a. Some factors affecting cyclic undrained triaxial strength of sand. Soils and Foundations. **26**(3): 99-116.

Tatsuoka, F., Ochi, K., Fujii, S. and Okamoto, M. 1986b. Cyclic undrained triaxial and torsional shear strength of sands for different sample preparation methods. Soils and Foundations. **26**(3): 23-41.

Tatsuoka, F., Kato, H., Kimura, M. and Pradhan, T.B.S. 1988. Liquefaction strength of sands subjected to sustained pressure. Soils and Foundations. **28**(1): 119-131.

Toki, S., Tatsuoka, F., Miura, S., Yoshimi, Y., Yasuda, S. and Makihara, Y. 1986. Cyclic undrained triaxial strength of sand by a co-operative test program. Soils and Foundations. **26**(3): 117-128.

Tanaka, Y., Kudo, K., Yoshida., Y., and Ikemi, M. 1987. A study on the mechanical properties of gravel – Dynamic properties of reconstituted sample. Res. Rep. No. U87019, Centr. Res. Inst. of Electric Power Industry, Akibo, Japan (in Japanese).

Triantafyllidis, Th., Wichtmann, T. and Niemunis, A. 2004. On the determination of cyclic strain history. *In* Proceedings of the Intern. Conf. on Cyclic Behaviour of Soils and Liquefaction Phenomena, CBS04, Bochum, Germany, pp. 371-387, A.A. Balkema Publishers, *Ed. by* Th. Triantafyllidis.

Vaid, Y.P. and Chern, J.C. 1983. Effect of static shear on resistance to liquefaction. Soils and Foundations, **23**(1): 47-60.

Vaid, Y.P. and Finn, W.D.L. 1979. Static shear and liquefaction potential. ASCE, J. Geotech. Eng., **105**(10): 1233-1246.

Vaid, Y.P., Sivathayalan, S. and Stedman, D. 1999. Influence of specimen reconstitution method on the undrained response of sand. ASTM Geotech. Testing J. **22**(3): 187-195.

Wijewickreme D., Sriskandakumar, S. and Byrne, P.M. 2004. Characterization of cyclic loading of air-pluviated Fraser River sand for validation of numerical models. www.civil.ubc.ca/liquefaction/

Wijewickreme D., and Sanin, M. 2005. Some observations on the cyclic loading response of a natural silt. In Proceedings of the XVI ICSMGE, Osaka, pp. 627-631.

Wong., R.T., Seed, H.B. and Chan, D.K. 1975. Cyclic loading liquefaction of gravelly soils. ASCE, J. Geotech. Engrg. **101**(6): 571-583.

Yoshimi, Y., Tokimatsu, K. and Ohara, J. 1994. In situ liquefaction resistance of clean sands over a wide density range. Geotechnique **44**(3): 479-494.

Laurits Bjerrums Minnefond

Statutter

§ 1 Opprettelse

Laurits Bjerrums minnefond er opprettet av Norsk geoteknisk forening, dels ved egne midler, og dels ved gaver fra private firmaer og offentlige institusjoner, samt fra enkeltpersoner.

§ 2 Formål

Fondets avkastning skal benyttes til å fremme geoteknisk forskning og stimulere det geotekniske miljø ved følgende tiltak:

(a) Laurits Bjerrums ærespris tildeles for et fremragende enkeltarbeid, eller for flere betydelige arbeider som sammen har fremmet faget geoteknikk og fundamentering.

(b) Laurits Bjerrums stipendium benyttes fortrinnsvis til å stimulere yngre, lovende geoteknikere til forskning innen faget.

(c) Laurits Bjerrums minneforedrag holdes av fremstående geoteknikere som inviteres og honoreres.

§ 3 Styre

Fondets midler forvaltes av et styre på 3 medlemmer valgt av generalforsamlingen i Norsk geoteknisk forening for en periode på 5 år, med mulighet for gjenvalg av de enkelte styremedlemmer én gang. Norsk geoteknisk forenings sekretær, kasserer og revisor fungerer som sådanne også for fondsstyret. Fondsstyret skal holde minst ett møte pr. år. Sekretæren innkaller til møtene og deltar i disse.

Fondsstyret tar avgjørelser i alle saker som vedrører bruk av fondets avkastning til ovennevnte formål Resultatet av avgjørelsen meddeles til Norsk geoteknisk forening som skal være arrangør ved minneforedragene og ved utdeling av ærespris og stipendium.

§ 4 Anvendelsesprinsipp

Anvendelsen av fondets avkastning skal så vidt mulig skje i Laurits Bjerrums ånd. Regelmessighet og rutine ved utdelingen bør vike prioritet for originalitet og oppfinnsomhet. Det eksepsjonelle skal honoreres fremfor mengde, og ved de respektive seremonier og tilstelninger skal det legges vekt på å skape særpreg og festivitas.

§ 5 Statuttendringer

Bestemmelsene i disse statutter kan etter år 2000, endres av Norsk geoteknisk forening i henhold til foreningens egne statutter. Fondsstyret skal på forhånd enstemmig ha erklært seg enig i endringsforslaget.

Statutter vedtatt av Norsk geoteknisk forenings generalforsamling 18. september 1973